

UCSF

UC San Francisco Electronic Theses and Dissertations

Title

New insights into the regulation of the Anaphase Promoting Complex

Permalink

<https://escholarship.org/uc/item/3b06k775>

Author

Foe, Ian Thomas

Publication Date

2012

Peer reviewed|Thesis/dissertation

New Insights into the regulation of the Anaphase Promoting Complex

by

Ian Thomas Foe

DISSERTATION

Submitted in partial satisfaction of the requirements for the degree of

DOCTOR OF PHILOSOPHY

in

Genetics

in the

GRADUATE DIVISION

of the

UNIVERSITY OF CALIFORNIA, SAN FRANCISCO

This work is dedicated to my family and my wonderful girlfriend

Acknowledgements

I would like to thank my graduate mentor David P. Toczyski. He has been instrumental in my growth as a scientist and as a person. I would also like to thank my lab who has been equally important in my development. In addition thanks must be given to my thesis committee members Dave Morgan and Carol Gross. I must also thank Scott Foster and Ellen Edenberg for the wonderful and fruitful collaborations that I have had during my time at UCSF. I would also like to acknowledge my family their support has been crucial throughout the years. Lastly I need to thank my girl friend Anna Reade (the smalls) who every day I love more than the last.

Scott A. Foster and Stephanie K. Cheung have all contributed to work in this thesis.

Parts of the General Introduction were taken from a previously published work the reference for which is below

Foe, I. and Toczyski, D.P. (2011). “A new look for the APC” *Nature*. **470**, 182-183

The original manuscript can be found here

<http://www.ncbi.nlm.nih.gov/pubmed/21307929>

The first chapter of this work and the figures have been previously published the reference is below.

Foe, I.T., Foster, S.A., Cheung, S.K., Deluca, S.Z., Morgan, D.O., Toczyski, D.P. (2011).

Ubiquitination of Cdc20 by the APC occurs through an intramolecular mechanism. *Curr Bio*. **27**, 1870-1877.

The original publication can be found at

<http://www.ncbi.nlm.nih.gov/pubmed/22079111>

Abstract

New insights into the regulation of the Anaphase Promoting Complex

Ian Thomas Foe

Proteolysis of cell cycle regulators is essential for transit through the cell cycle. Much of this proteolysis is mediated by a process called ubiquitination. Ubiquitination occurs via an enzyme cascade and culminates in the covalent attachment of ubiquitin moieties to a substrate molecule. Ubiquitin ligases are essential for ubiquitination and select the substrates for ubiquitination. An example of an Ubiquitin ligase involved in cell cycle control is the Anaphase Promoting Complex (APC). The APC is essential for the proteolysis of several distinct molecules at the transition from metaphase to anaphase. The destruction of these molecules initiates a series of events that result in the onset of anaphase. The APC is critical for cell cycle progression, and likely because of this evolution has created a myriad of ways to regulate its activity including; transcriptional regulation, proteolysis, localization, and post-translational modification. Work presented here discusses novel mechanisms for regulating the APC. The first chapter looks at how Cdc20 one of the APC's mitotic substrate adaptors is proteolysed during the cell cycle. This work shows that Cdc20 is turned over via an auto ubiquitination mechanism, and this mechanism is likely influenced by substrate concentration. Chapter 2 focuses on the DNA damage checkpoint and how it directly phosphorylates Apc1 a scaffolding subunit of the APC. Importantly work presented here suggests that this phosphorylation may inhibit APC activity during DNA damage helping to enforce the arrest in metaphase seen on DNA damage.

| Table of Contents | Page |
|-------------------------------------------------------------------------------|-------------|
| Dedication | iii |
| Acknowledgments | iv |
| Abstract | vi |
| List of Figures | viii |
| General Introduction | 1 |
| Chapter 1: | 4 |
| Ubiquitination of Cdc20 by the APC occurs through an intramolecular mechanism | |
| Chapter 2: | 34 |
| Apc1 is target of the DNA damage checkpoint | |
| Work Cited | 63 |

| List of Figures | Page |
|--------------------------------------------------------------------------------------------------------------------------|-------------|
| Figure 1. | 25 |
| Cdc20 is turned over by the APC by Cdh1-dependent and Cdh1-independent mechanisms. | |
| Figure 2. | 26 |
| Cdc20 ubiquitination and turnover in <i>CDC20</i> , <i>CDH1</i> mutants. | |
| Figure 3. | 27 |
| The majority of Cdc20 turnover occurs by the Cdc20 ^{cis} mechanism. | |
| Figure 4. | 28 |
| Cdc20 levels oscillate with the cell cycle in a Cdh1- and transcription-independent manner. | |
| Figure 5. | 29 |
| Cdc20 ^{cis} mechanism is inhibited by high substrate concentrations. | |
| Figure 6. | 30 |
| Model demonstrating how Cdc20 ^{cis} may be regulated by substrate. | |
| Supplemental Figure 1. | 32 |
| <i>In vitro</i> ubiquitination of Cdc20 C-box and IR mutants by Cdh1, and turnover of Cdc20 C-box mutants <i>in vivo</i> | |
| Supplemental Figure 2. | 33 |
| Facs profiles for <i>cdc15-1</i> arrest release experiments (Figure 5) | |
| Figure 7. | 57 |
| Diagram of the APC and the DNA damage checkpoint. | |
| Figure 8. | 58 |
| Apc1 is target of the DNA damage checkpoint. | |
| Figure 9. | 59 |
| APC substrates are stabilized during DNA damage. | |

| | |
|------------------------------------------------------|----|
| Figure 10. | 60 |
| Cdc20 stability during damage is dependent on Rad53. | |
| Figure 11. | 61 |
| Apc1 domain mapping. | |
| Figure 12. | 62 |
| Model for how damage may inhibit APC activity. | |

General Introduction

Ubiquitin-mediated proteolysis is a key regulatory mechanism of the cell cycle. Ubiquitination occurs via an enzyme cascade culminating in the attachment of ubiquitin chains to target proteins. Substrate selection from the cellular protein pool is accomplished by an enzyme called an ubiquitin ligase. One of the most complex ligases known is the Anaphase Promoting Complex (APC), a 1.5 MDalton assemblage of 1-2 copies of each of 13 different subunits [1, 2], as well as two diffusible mitotic adaptors [3-5]. One of the most important functions of the APC is promoting the transition from metaphase into anaphase. The APC accomplishes this through the controlled degradation of pds1 and the mitotic cyclins [6, 7] which lead to activation of the protease Esp1 and entry into anaphase [8].

Due to the importance of the APC in promoting this transition a large amount of work has been done to increase our understanding of this ligase. Previous molecular genetics and structural studies have demonstrated that while the APC is incredibly complex, its core can be broken down into 3 distinct subcomplexes [9, 10]. The APC is composed of a subcomplex called the platform (Apc1, Apc4 and Apc5), upon which the two additional subcomplexes, the TPR and the catalytic subcomplexes are attached [9, 10]. The TPR subcomplex contains homodimers of three (or four, in metazoans) subunits with tetratricopeptide (TPR) repeats (Cdc23, Cdc16 and Cdc27)[2, 11, 12], with the Cdc23 homodimer serving as the contact point with the platform region [9, 10]. The catalytic subcomplex contains the Cullin (Apc2) and Ring (Apc11) proteins, common to this class of ubiquitin ligases [9, 10]. It also contains Doc1 a subunit implicated in

substrate binding and is thought to form a co-receptor with the APC's substrate adaptors (Cdc20 and Cdh1) [9, 10, 13-15].

Cdc20 and Cdh1 are thought to function in a similar manner to each other. Each adaptor contains two APC binding motifs, the first of which is a C-terminal Isoleucine-Arginine motif referred to as the IR domain [16, 17]. The other motif that the activators use to bind to the APC is an N-terminal motif called the C-box [18]. In addition to its role in binding, the C-Box also appears to have a role in activating the APC towards its substrates though [19], the mechanism is poorly understood. Cdc20 and Cdh1, in addition to their APC binding motifs share a third motif called a WD40 domain. The WD40 domain is thought to bind degradation (degron) sequences in APC substrates [20]. There are many types APC degrons, the most common ones being the Destruction box (D-box) [21] and the KEN box [22].

The APC, and in particular its activators, are regulated in a variety of ways. An example is the regulation of Cdc20 transcription and protein levels. Cdc20 transcripts and protein levels oscillate throughout the cell cycle [23, 24]. Cdc20 transcription is shut off in G1, rises in late S phase, stays high throughout early mitosis and drops in late mitosis [23, 24]. Cdc20 protein levels follow a very similar pattern, with the APC itself driving Cdc20 ubiquitination in late mitosis and G1 [23-25]. Another example of APC regulation is the inhibition and degradation of Cdc20 during the spindle assembly checkpoint [26]. Recently, activator binding to the APC has been shown to be regulated by acetylation [27]. The APC is also regulated by phosphorylation. The phosphorylation of the TPR subcomplex is thought to promote Cdc20 binding to the APC [28], while the phosphorylation of Cdh1 is thought to inhibit the binding of Cdh1 to the APC [29, 30].

The work presented here investigates additional and novel means of APC regulation. Chapter 1 focuses on how Cdc20 is turned over by the APC. In this chapter we show that Cdc20 main form of turnover is not mediated by Cdh1 as previously thought. Instead, we show that the majority of Cdc20 turns over via an autoubiquitination mechanism. Importantly, we show that this mechanism is regulated throughout the cell cycle and that substrate concentration may influence this mechanism of Cdc20 turnover. In Chapter 2 we show that Apc1, a scaffolding subunit of the APC, is direct target of the DNA damage checkpoint. Importantly, we find that APC substrate turnover is inhibited during DNA damage in a DNA damage checkpoint dependent manner.

Chapter 1

Ubiquitination of Cdc20 by the APC occurs through an intramolecular mechanism

Summary

Background: Cells control progression through late mitosis by regulating Cdc20 and Cdh1, the two mitotic activators of the Anaphase Promoting Complex (APC). The control of Cdc20 protein levels during the cell cycle is not well understood.

Results: Here, we demonstrate that Cdc20 is degraded in budding yeast by multiple APC-dependent mechanisms. We find that the majority of Cdc20 turnover does not involve a second activator molecule, but instead depends on *in cis* Cdc20 autoubiquitination while it is bound to its activator-binding site on the APC core. Unlike *in trans* ubiquitination of Cdc20 substrates, the APC ubiquitinates Cdc20 independent of APC activation by Cdc20's C-box. Cdc20 turnover by this intramolecular mechanism is cell cycle-regulated, contributing to the decline in Cdc20 levels that occurs after anaphase. Interestingly, high substrate levels *in vitro* significantly reduce Cdc20 autoubiquitination. **Conclusion:** We show here that Cdc20 fluctuates through the cell cycle via a distinct form of APC-mediated ubiquitination. This *in cis* autoubiquitination may preferentially occur in early anaphase, following depletion of Cdc20 substrates. This suggests that distinct mechanisms are able to target Cdc20 for ubiquitination at different points during the cell cycle.

Introduction

Chromosome segregation is one of the most tightly regulated events in the dividing cell. Incorrect entry into anaphase can have catastrophic cellular consequences ranging from genomic instability to cell death. Anaphase is initiated by the Anaphase-Promoting Complex/Cyclosome (APC) [31, 32], an E3 ubiquitin ligase composed of at

least 13 core subunits [1, 33]. APC function is regulated by association with one of two activator subunits, Cdc20 or Cdh1 (also known as Hct1) [3-5]. These proteins are thought to function both in the binding of substrates to the APC [18] and APC activation [19]. Cdc20 associates with the APC in early mitosis, and triggers anaphase onset by promoting the destruction of a subset of mitotic cyclins and Securin (also known as Pds1) [6, 7], resulting in the activation of Esp1, and the separation of sister chromatids through cleavage of cohesion [8]. In late mitosis and G1, Cdh1 associates with the APC, promoting mitotic exit and maintaining low Cdk activity.

Both activators contain well-conserved motifs involved in APC and substrate binding (Figure 1A). APC binding is mediated by both a C-box motif within the activator's N-terminus [18] and a C-terminal Isoleucine-Arginine (IR) motif [16, 17] (Figure 1A). Substrate binding is mediated by a WD40 domain that is likely to interact directly with degradation signals found within substrates [20], the most common being the Destruction box (D-box) [21] and KEN-box [22]. Processive substrate ubiquitination has also been shown to require the core APC subunit Doc1 [16, 34], which is thought to function as a co-receptor for the D-box in conjunction with the WD40 of Cdc20/Cdh1 [14, 15].

The two mitotic APC activators are thought to function analogously, but they are regulated in distinct ways. While Cdh1 protein and transcript levels are constitutive, Cdc20 transcription and protein levels both oscillate throughout the cell cycle [23]. Cdc20 is absent in G1, but begins to accumulate in late S phase, its peak coinciding with the initiation of anaphase. Cdh1 is thought to bind an N-terminal D-box within Cdc20, leading to the destruction of Cdc20 in late mitosis and G1 [35-37]. However, while Cdh1-

mediated turnover of Cdc20 is likely important, several studies have suggested that Cdc20 is also turned over by Cdh1-independent mechanisms [10, 23, 38]. Regulation of Cdc20 levels is very important, as high-level over-expression of Cdc20 is lethal [39] and as little as three-fold over-expression of Cdc20 is sufficient to override the spindle assembly checkpoint [40].

Previously, we found that deletion of Cdc20's IR domain caused a strong accumulation of Cdc20 *in vivo* [10], which is inconsistent with Cdc20 simply being a passive Cdh1 substrate. Here, we show that Cdc20 turnover is fully APC-dependent, but does not depend on a second activator molecule. While Cdc20 can be targeted by the APC associated with either Cdh1 or, more poorly, by a second Cdc20 molecule (i.e. *in trans* turnover), we find that most turnover *in vivo*, and ubiquitination *in vitro*, is promoted by direct association with the APC (*in cis* turnover) (Figure 1B). Consistent with this model, we show that processive ubiquitination of Cdc20 does not require Doc1. Importantly, we find that Cdc20 levels oscillate independently of *CDC20* transcription and Cdh1 activity, implying that the *in cis* autoregulation of Cdc20 turnover changes during the cell cycle. Additionally this regulation can be influenced by the presence of APC^{Cdc20} substrates. These findings uncover another mechanism by which the activity of the APC is tightly controlled during the cell cycle.

Results

Cdc20 turnover depends on the APC

Cdc20 is thought to be destroyed by both APC-dependent mechanisms [23, 24, 41] and APC-independent mechanisms [41]. However, previous experiments suggesting

APC-independent Cdc20 turnover were performed with temperature-sensitive APC mutants, which do not necessarily eliminate all APC function. While the APC is normally essential, we have previously shown that deletion of genes encoding two Cdc20 substrates, Pds1 and Clb5, combined with 10-fold over-expression of the Cdk inhibitor Sic1 (*SIC1^{10x}*), allows cells to survive in the absence of the APC [42]. To determine whether Cdc20 turnover is dependent upon a functional APC, we examined Cdc20 turnover in an *apc11Δ pds1Δ clb5Δ SIC1^{10x}* strain. Deletion of *APC11*, which encodes the essential RING finger subunit of the APC [43], abolishes APC activity in the cell. We found that, as with the known APC substrate Clb2 [44], turnover of Cdc20 was eliminated in the *apc11Δ* strain (Figure 1C). This strongly suggests that, under normal conditions, the majority of Cdc20 turnover depends on APC activity.

We postulated that there could be three modes of APC-dependent Cdc20 turnover (Figure 1B). First, as previously suggested, Cdh1 bound to the APC as an activator could recognize Cdc20 as a substrate through Cdc20's D-box (Cdh1^{trans})[35-37]. However, we found previously that while Cdc20 levels were slightly increased in *cdh1Δ* cells, they were more dramatically increased in *Apc⁻* cells [10], suggesting that the APC targets Cdc20 by Cdh1-independent mechanisms as well. Consistent with this, we observed APC-dependent ubiquitination of Cdc20 both in the presence and absence of Cdh1 *in vitro* (Figure 1D).

There are two distinct mechanisms by which Cdh1-independent ubiquitination could occur. The first is similar to the Cdh1^{trans} mechanism. Here, one molecule of Cdc20 associates with the APC as an activator and this APC-Cdc20 complex binds a second Cdc20 molecule as a substrate through a WD40/D-box interaction (Cdc20^{trans},

Figure 1B). Alternatively, a single Cdc20 molecule bound to the APC as an activator could be ubiquitinated directly by the APC (Cdc20^{cis}, Figure 1B).

Contribution of the Cdh1-dependent and independent mechanisms to Cdc20 turnover

We found previously that mutation of Cdc20's IR motif increased steady-state Cdc20 levels [10], consistent with a Cdh1-independent mechanism for Cdc20 turnover. This increase in steady-state level is higher than that observed for wildtype Cdc20 in a *cdh1Δ* strain, suggesting that the Cdh1-independent mechanism is responsible for the majority of Cdc20 turnover (Figure 2A, lanes 5&9) [10]. The IRΔ and *cdh1Δ* double mutant was more stable than either single mutant, consistent with multiple mechanisms controlling Cdc20 stability (Figure 2A lanes 5-16). Since mutation of the IR decreases Cdc20 binding to the APC (data not shown), both Cdc20^{trans} and Cdc20^{cis} could, in principle, be affected. Consistent with this idea, we found that mutation of the IR had no effect on Cdh1-dependent ubiquitination *in vitro* (Supplementary Fig. 1A) but greatly inhibited autoubiquitination (Figure 2B, lanes 9-12).

To further assess the contribution of the Cdh1^{trans} mechanism in isolation, we sought to create a Cdc20 mutant that was defective in binding to the APC as an activator, but could be bound as a substrate through its D-boxes. The observation that mutation of Cdc20's IR motif has no obvious growth phenotypes is consistent with it only having a partial effect on Cdc20 binding to the APC. Mutation of C-box, however, is lethal and decreases Cdc20 binding to the APC [10, 18], suggesting that C-box mutations greatly reduce interaction with the APC. Therefore, we expected a C-box mutation to eliminate

Cdc20^{cis} and Cdc20^{trans} mediated turnover. The minimal conserved sequence of the C-box in both Cdc20 and Cdh1 is DRYIP [18]. Previously, we characterized two C-box mutants, a weaker *cdc20-I147A,P148A* allele and a stronger *cdc20-R145D* allele (which did not translate well *in vitro*) [10]. We examined the turnover of Cdc20-R145D in a *cdh1Δ* strain. Surprisingly, while the known Cdc20 substrate Dbf4 was stabilized, the Cdc20-R145D protein was still turned over rapidly, although there was an increase in steady-state levels (Figure 2C lanes 4-9 and Supplementary Fig. 1B). It was possible that this mutation did not entirely eliminate C-box function, so we also analyzed a *cdc20-D144R, R145D* double mutant. This mutant turned over with similar kinetics to the *cdc20-R145D* allele (Supplementary Fig. 1C).

We also observed that the *I147A, P148A* C-Box mutant had a larger effect than the IR mutation on securin ubiquitination *in vitro* (Figure 2D, lanes 7-12). Yet the defect observed with the same C-box mutation is less severe than that observed with the IR mutant in autoubiquitination activity (Figure 2B, lanes 5-12). Thus, while the C-Box is essential for APC function *in vivo*, considerable Cdc20 turnover occurs when the C-box is mutated. Our results, together with previous evidence that the C-box, but not the IR, is essential for viability, indicates that the C-box is more important than the IR motif for substrate turnover and less critical for Cdc20 autoubiquitination.

Since neither the IR nor C-box mutation alone eliminated Cdh1-independent turnover, we generated a C-box, IR double mutant. Cdc20-IR, R145D should not be able to interact with the APC as an activator and therefore should eliminate both the Cdc20^{trans} and Cdc20^{cis} mechanisms of turnover. Consistent with this, the Cdc20-IR, R145D mutant was strongly stabilized in a *cdh1Δ* strain, but could be turned over in a *CDH1* strain

(Figure 3A, lanes 7-9 and 13-15). Similarly, we detected ubiquitination of a Cdc20-C-box-IR mutant in the presence of Cdh1 *in vitro* and this activity was entirely D-box-dependent (Figure 3B, lanes 1-6). These results are consistent with previously suggested model that Cdh1 can target Cdc20 [35-37]. However, the dramatic increase in steady-state levels and the relatively slow rate of turnover in the Cdh1^{trans}-only strain suggests that Cdh1-dependent turnover likely contributes to a small portion of normal Cdc20 turnover (Figure 3A, lanes 7-9).

We next sought to investigate if the Cdc20^{trans} mechanism makes any contribution to Cdh1-independent turnover. We generated a *cdh1Δ* strain containing a wildtype copy of *CDC20* and the *cdc20-IR, R145D* allele at a second locus. Turnover of Cdc20-IR, R145D should be defective in both the Cdh1^{trans} and Cdc20^{cis} mechanisms in this strain and should therefore be turned over exclusively by Cdc20^{trans}. This Cdc20-IR, R145D mutant was slightly more stable than that observed in the Cdh1^{trans}-only strain, suggesting that the Cdc20^{trans} mechanism does occur, but likely contributes very little to Cdh1-independent turnover (Figure 3A, lanes 10-12). To further characterize the Cdc20^{trans} mechanism, we tested whether a wildtype copy of Cdc20 can ubiquitinate this double mutant *in vitro*. We detected very little ubiquitination of this mutant in the presence of a wildtype copy of Cdc20 and the little stimulation seen over background was D-box-dependent (Figure 3C, lanes 4-6 & 10-12). Interestingly, while this D-box appears Cdh1-specific in terms of targeting Cdc20 as a substrate *in vitro*, we did see a slight defect with this mutant both in direct binding to the APC and in targeting Securin for ubiquitination *in vitro*, suggesting that Cdc20's D-box may have an additional function (data not shown).

Given that total Cdc20 turnover appeared significantly faster than turnover via either Cdc20^{trans} or Cdh1^{trans}, we examined the contribution of the Cdc20^{cis} mechanism using an allele of Cdc20 that could only be bound to the APC as an activator and not as a substrate. We generated a *cdh1Δ* strain in which the only copy of Cdc20 is mutated at its first D-box (*cdc20-DB*), and thus cannot function as a substrate in a Cdc20^{trans} reaction. In this strain, where only Cdc20^{cis} turnover occurs, Cdc20 turnover is quite fast, and steady-state Cdc20 levels are low, similar to those in a *cdh1Δ* strain where both Cdh1-independent mechanisms can occur (Fig. 3D, lanes 1-8). These data suggest that Cdc20^{cis} is the dominant form of Cdc20 turnover, with the contribution of Cdc20^{trans} being very small (Figure 3D, lanes 9-12).

To determine the extent to which the first D-box mutation eliminates Cdc20^{trans} turnover *in vivo*, we examined its effect in our strain that uses Cdc20^{trans} exclusively (see Figure 3A, lanes 10-12). We found that Cdc20-IR, R145D, DB was extremely stable in a *CDC20 cdh1Δ* strain, although a very low level of turnover did occur (Figure 3D, lanes 13-16). Mutation of a second N-terminal D-box had no additional effect (data not shown). Thus, the D-box mutation eliminated *in trans* turnover, consistent with previous reports [23, 24]. These data suggest that Cdc20^{cis} is the dominant form of Cdc20 turnover, with the contribution of Cdc20^{trans} being very small (Figure 3D, lanes 5-8 & 9-12).

The nonessential APC subunit Doc1 (APC10) is thought to interact directly with the D-box of substrates and enhance processivity by limiting the dissociation rate of the substrate [14, 16, 34]. Deletion of this subunit or mutation of 4 residues (Doc1-4A) within its putative substrate binding site leads to a decrease in the number of ubiquitins

conjugated to the substrate, as visualized by a significant decrease in higher molecular weight substrate-ubiquitin bands and accumulation of mono-ubiquitinated substrate (Figure 3E, lanes 1-8)[14]. Cdc20 contains a D-box that has been shown to be important in Cdh1-dependent ubiquitination [23]. We tested whether a Doc1/D-box interaction was required for processive ubiquitination of Cdc20 *in vitro* in the absence of Cdh1. Unlike our results with all other substrates tested, mutation of Doc1 had no effect on the processivity of this reaction. Doc1 and Doc1-4A had nearly identical activity towards Cdc20 (Figure 3E, lanes 9-16), implying that Doc1 is not required for Cdh1-independent ubiquitination of Cdc20. These data strongly suggest that Cdc20 is not ubiquitinated by the APC as a canonical substrate, and can best be explained by the Cdc20^{cis} mechanism of autoubiquitination.

Cdc20 levels oscillate independently of Cdh1 and Cdc20 transcriptional oscillation

Cdh1 activity is cell-cycle regulated, which contributes to Cdc20 periodicity. We sought to determine if Cdh1-independent mechanisms are also important for oscillations in Cdc20 levels. Since *cdh1Δ* cells do not arrest well in alpha factor, we examined Cdc20 levels through the cell cycle using *cdh1Δ cdc15-2* cells. Cells were arrested at the non-permissive temperature in anaphase and released into the permissive temperature. Consistent with a recent report, we found that Cdh1 is not necessary for Cdc20 levels to fluctuate with the cell cycle [38] (Figure 4A, Supplementary Fig. 3A).

To examine the extent to which oscillations in *CDC20* transcription contribute to the fluctuation of Cdc20 levels, we generated a strain with *CDC20* under the control of a constitutive promoter (*TEF1p*). Cdc20 levels were still periodic in this strain. Moreover,

Cdh1 was not required for this periodicity (Figure 4B, Supplementary Fig. 3B). While Cdh1-dependent turnover of Cdc20 and cell cycle-regulated transcription both contribute to Cdc20 cycling, Cdh1-independent turnover mechanisms appear to add significantly to Cdc20 oscillation.

Substrates inhibit Autoubiquitination

If Cdc20 targets itself while bound to the APC as an activator, then how does the cell maintain Cdc20 levels sufficient to trigger anaphase? We tested the possibility that the binding of substrates to Cdc20 might inhibit autoubiquitination, maintaining Cdc20 stability until its targets are depleted in anaphase. We generated an N-terminal fragment (aa 1-110) of budding yeast securin, containing the characterized destruction motif [6]. As expected for a competitive inhibitor, this fragment potently inhibited securin ubiquitination ($IC_{50} \sim 200$ nM) (Figure 5A). A 10 μ M concentration of the securin fragment completely inhibited ubiquitination of securin (Figure 5A). This concentration of the fragment also inhibited the total activity and processivity of Cdc20 autoubiquitination (Figure 5B). These results support the notion that substrate blocks autoubiquitination, prolonging Cdc20 levels in the cell until substrates are depleted (Figure 6).

Discussion

One of the first APC substrates to be identified was its own activator, Cdc20, hinting at the existence of autoregulation [23, 24]. Initial reports suggested that Cdc20 behaved similarly to other APC substrates, being targeted in part via a different activator

(Cdh1) through Cdc20's D-box [35-37]. Interestingly, we show here that, unlike other APC substrates, Cdc20 is largely targeted for destruction by the APC through an autoubiquitination mechanism that occurs when Cdc20 is bound to the APC as an activator. Importantly, this mechanism appears to be regulated throughout the cell cycle, and may be influenced by the presence or absence of substrates.

The observation that Cdc20 turnover was only partially reduced in conditional APC mutants led some authors to speculate that the residual turnover observed might be mediated by an APC-independent pathway. Our work in a strain that permits the deletion of the *APC11* gene shows that in unperturbed cells, Cdc20 is turned over solely by the APC. This discrepancy is likely due to the fact that conditional alleles may not be completely null for APC activity, whereas deletion of the gene encoding the catalytic subunit (*APC11*) eliminates activity completely.

APC^{Cdh1} has long been assumed to be the APC complex that targets Cdc20 for destruction (Cdh1^{trans}, Figure 1B) [22, 35-37]. However, deletion of *APC11* leads to much greater steady-state levels of Cdc20 than deletion of *CDH1*, suggesting the existence of other APC-mediated mechanisms [10]. This suggests two obvious models for turnover. First, Cdc20 bound to the APC as an activator could recognize another molecule of Cdc20 leading to ubiquitination of the substrate Cdc20 (Cdc20^{trans}, Figure 1B). In this case, the substrate Cdc20 should behave similarly to other Cdc20 substrates. Alternatively, Cdc20 may bind to the APC as an activator and this binding alone may be sufficient for autoubiquitination (Cdc20^{cis}, Figure 1B). To evaluate the relative contributions of the three possible modes of Cdc20 turnover, we generated strains in which only one mechanism of turnover was possible and performed *in vitro* experiments

with similar perturbations. These experiments strongly suggested that Cdc20^{cis} is the predominant form of Cdc20 turnover.

Previous work showed that Cdc20 not only recruits substrates to the APC, but also serves to activate the APC, since its presence was also required for the ubiquitination of the APC substrate Nek2A, which can bind the APC independently of an activator [19, 45]. Importantly, these results suggested that an N-terminal fragment of Cdc20 containing the C-box was sufficient to activate the APC toward Nek2A, and that the C-box was required for this activation [19]. Interestingly, we find that a Cdc20 C-box mutant, which does not support viability and is unable to drive Dbf4 turnover in vivo [10](Fig. 2C), is still targeted for turnover by the APC, although its turnover is compromised. This result suggests that the C-box is not absolutely required for APC activity, but is specifically required for stimulating APC activity towards other APC substrates, potentially by properly orientating either the substrate and or the catalytic arm of the APC so substrate ubiquitination can occur. Interestingly, deletion of the C-terminal IR domain, which does not result in a growth defect, has a significant effect on Cdc20 turnover, slightly greater than the defect seen for the lethal C-box mutant. The IR domain has been shown to interact with Cdc27, the terminal subunit of the TPR arm [10, 17, 46]. The non-essential nature of the IR-Cdc27 interaction could suggest that it is an intermediate in the reaction mechanism when Cdc20 is particularly susceptible to autoubiquitination. Consistent with this observation, this interaction is not required for the processive ubiquitination of other APC substrates [46]. However, the lack of affinity provided by the Cdc27-IR interaction is compensated by an interaction between the activator, substrate, and Doc1 on the APC core. However, autoubiquitination does not use

Doc1, possibly, making the affinity provided by the Cdc27-IR interaction more important.

The discovery that Cdc20 is targeted for turnover by Cdh1, which is itself cell-cycle regulated, suggested a mechanism by which Cdc20's cyclical expression could be achieved. Work from the Cross lab [38] and from experiments presented here suggests that Cdh1 may contribute to but is not necessary for Cdc20's cell cycle oscillation. However, previous work [23] suggested that oscillation in Cdc20 levels is also achieved by transcriptional regulation. *CDC20* is a member of the *CLB2* cluster of genes [47], whose transcription is under the control of Fkh2/Ndd1 [48, 49]. The observation that Cdc20 levels still oscillate in cells that express *CDC20* under a constitutive promoter (*TEF1p*) in the absence of Cdh1 implies an additional cell cycle regulated mechanism. This is strong evidence that regulation of the Cdc20^{cis} mechanism we observe is sufficient to drive the oscillatory behavior of Cdc20 through out the cell cycle.

Previous work has shown that phosphorylation of the TPR subunits (Cdc27, Cdc16, and Cdc23) by the Cyclin-Dependent Kinase (CDK) increases the affinity of Cdc20 for the APC [28]. It is possible that these phosphorylations are regulating the Cdc20^{cis} mechanism. However, these phosphorylations promote Cdc20 binding to the APC, and occur when CDK activity is high. If these phosphorylations are promoting the Cdc20^{cis} turnover during the cell cycle, we would expect to see the lowest Cdc20 levels when CDK activity is highest. However, we observe that the lowest Cdc20 levels occur during the G1 phase of the cell cycle, when CDK activity is lowest. Alternatively, phosphorylation of the TPR proteins may cause Cdc20 to bind in a slightly different position on the APC, which may inhibit the Cdc20^{cis} mechanism.

These data suggest the following model. The APC is hyperphosphorylated in early mitosis, which increases its affinity for Cdc20. As APC^{Cdc20} runs out of substrates, Cdc20 begins to autoubiquitinate, constituting the majority of the late mitotic turnover. This model for the regulation of Cdc20 stability by the presence of substrates (Figure 6) is similar to that put forth for the ubiquitin conjugase Ube2C [50]. As cells exit mitosis, APC becomes dephosphorylated and Cdh1 becomes active, thus removing residual Cdc20. Additionally, our model for substrate inhibition of Cdc20 turnover may explain why it is advantageous for the cell to have Cdc20 binding to the APC strongly enhanced by the presence of substrates [46, 51]. In this way, Cdc20 would be unlikely to be prematurely degraded when substrates are present.

Interestingly, Cdc20 turnover has been shown to increase in the presence of spindle poisons. This turnover is dependent on an intact Spindle Assembly Checkpoint (SAC) [40]. The exact mechanism for this turnover is unknown, but it will be interesting to determine the mechanism for Cdc20 turnover during SAC activation.

Methods

Yeast Methods

Yeast were grown in Ym-1 media [52] and 2% dextrose. All cells were grown at 23°C unless otherwise noted. Cdc20 integrating plasmid was created by cloning Cdc20 and its promoter into pRS306 using standard techniques. Mutations to pRS306-Cdc20 were accomplished using quick change mutagenesis. Cdc20 plasmids were integrated at the *URA3* locus into derivations of 3 strains: *pds1Δ clb5Δ SIC1^{10x} cdc20Δ cdh1Δ*, *pds1Δ clb5Δ SIC1^{10x} cdc20Δ CDH1*, or *pds1Δ clb5Δ SIC1^{10x} CDC20 cdh1Δ*. All strains created

in this manner were checked for single integration by southern blot. Replacement of the *CDC20* promoter with *TEF1p* was accomplished using standard PCR-based techniques, as was deletion of *CDH1* and mutation of Cdc20's IR motif in Figure 2A.

Half-life assays

Cells were grown to saturation, diluted and allowed to grow for at least 2 doublings to an OD between 0.6 and 1.0. 6 ODs of cells were collected for the zero time point. Cell pellets were washed with 1 ml cold H₂O and frozen on dry ice. Cycloheximide was added to cultures for a final concentration of 50 µg/ml media. 6 ODs of cells were collected for each time point as indicated. Cell pellets processed as described below.

***cdc15-2* arrest and release**

Cells were grown to saturation, then diluted to an OD of 0.3 and allowed to grow to an OD between 0.6 and 1.0. 6 ODs of cells were collected as described above for an asynchronous sample. Cells were diluted to an OD of 0.5 and placed at 37°C for 3 h. Cells were examined under a microscope to confirm anaphase arrest. 6 ODs of cells were collected for the zero time point, as described above. Cells were then released into media at 23°C at an OD of 0.6, and 6 ODs of cells were collected at time points indicated. Cells were collected for flow cytometry at every time point and processed [53].

Western blots

Cell pellets were processed as follows. Cell pellets were thawed in boiling sample buffer (50mM Tris pH 7.5, 5% SDS, 5 mM EDTA, 10% Glycerol, 0.5% BME, 0.1 µg/ml

pepstatin A, 0.1 $\mu\text{g/ml}$ leupeptin, 0.1 $\mu\text{g/ml}$ bestatin, 0.1 mM Benzamidine, 5 mM NaF, 0.5 mM Na_3VO_4 , 40 mM β -glycerophosphate, 1 mM PMSF). Cells were boiled for 5 min, followed by bead-beating three times, 30 s each, and then boiled again for 5 min for SDS-PAGE and transfer to nitrocellulose. Western blots were performed with low salt PBST (15 mM NaCl, 1.3 mM NaH_2PO_4 , 5.4 mM Na_2HPO_4 , 0.05% Tween pH 6.8). All primary antibody incubations were performed overnight in 5% milk and low salt PBST unless otherwise noted. Antibodies were used as follows: Cdc20 (yC-20) from Santa Cruz at 1:1000, Cdc28 from Santa Cruz (yC-20) at 1:1000, Dbf4 (yN-15) from Santa Cruz at 1:500, Clb2 (y180) from Santa Cruz 1:1000 (Figure 4B), Cdc6 9H8/5 from Abcam at 1:2000.

APC Assays

APC was purified from a *TAP-CDC16*, *cdh1 Δ* strain. E1, E2 (Ubc4), APC, and Cdh1 were expressed and purified as previously described [14, 54]. ZZ-tagged Cdc20 wildtype and mutants were transcribed and translated *in vitro* with TnT Quick Coupled Transcription/Translation Systems (Promega) either in the presence of ^{35}S -methionine or unlabeled methionine. Briefly, APC assays were performed by first charging the E2 in the presence of E1 (Uba1, 300 nM), E2 (Ubc4, 50 μM), Methyl-Ubiquitin (Boston Biochem, 150 μM), and ATP (1 mM) for 20 min. E1/E2(Ubc4)/Methyl-Ubiquitin mix was added to APC (1-5 nM), ZZ-Cdc20 purified from reticulocyte lysate using IgG beads and cleaved using TEV protease, and Securin purified similarly from reticulocyte lysate. In Figure 2D, APC, Cdc20 and Securin were preincubated to increase the amount of activity observed for the mutants. For Figure 5A & B, His-tagged Securin (aa1-110) was

expressed in bacteria and purified using Ni-NTA resin. After TEV protease cleavage to remove the His6-tag, the protein was further purified using cation exchange and size exclusion chromatography. APC, Cdc20, and Securin (aa1-110) were preincubated before adding IVT Securin and E1/E2(Ubc4)/Methyl-Ubiquitin mix or E1/E2(Ubc4)/Methyl-Ubiquitin mix alone. All reactions were stopped by the addition of sample buffer, separated by SDS-PAGE, and visualized and quantified with a Molecular Dynamics PhosphorImager and ImageQuant (Amersham Biosciences/GE Healthcare).

Acknowledgements:

We would like to thank C. Carroll, N. Lyons, M. Lopez, G. Yaakov, L. Holt, M. Rodrigo-Brenni, M. Matyskiela, E. Edenberg, M. Downey, T. Berens J. Lopez-Mosqueda, D. Simsek and J. Benanti for their input and advice during this project. Additionally, we would like to thank N. Lyons, E. Edenberg, and M. Downey for reading and commenting on the manuscript. This work was supported by funding from the National Institute of General Medical Sciences to D. P. T. (GM070539) and D.O.M. (GM053270).

Figure Legends

Figure 1. Cdc20 is turned over by the APC by Cdh1-dependent and Cdh1-independent mechanisms. **(A)** Diagrams of Cdc20 and Cdh1. Red, purple, blue and green boxes represent the D-boxes, the C-box, the WD40, and the C-terminal IR, respectively. **(B)** Three possible mechanisms of Cdc20 turnover: Cdh1^{trans}, Cdc20^{trans}, Cdc20^{cis}. **(C)** Asynchronous *pds1Δ clb5Δ SIC1^{10x}* cells were collected at indicated time points after

cycloheximide addition. Blots were probed with antibodies against Cdc20, Clb2 and Cdc28, which served as a loading control. **(D)** APC immunopurified from TAP-Cdc16 lysates in a *cdh1Δ* background was used in ubiquitination reactions using *in vitro* translated (IVT) ZZ-tagged ³⁵S-Metionine-Cdc20 purified from rabbit reticulocyte lysates using IgG beads. APC (++) and (+) are 5 nM and 1 nM final concentrations, respectively. Controls show the dependence on the presence of exogenous E1/E2(Ubc4)/Methyl-Ubiquitin mix and the APC.

Figure 2. Cdc20 ubiquitination and turnover in *CDC20*, *CDH1* mutants. **(A)**

Asynchronous *PDS1 CLB5 SIC1* cells were treated with cycloheximide and samples were analyzed as in Figure 1C. Cdc20-IR denotes the Cdc20-ΔIR allele. **(B)** ZZ-tagged ³⁵S-

Cdc20 wildtype, C-Box mutant (I147A, P148A) or IR mutant (I609A, R610A) were generated by IVT and incubated with APC (5 nM) and E1/E2(Ubc4)/Methyl-Ubiquitin mix for the indicated times. Quantifications are shown below. **(C)** Asynchronous *pds1Δ clb5Δ SIC1^{10x}* cells were treated with cycloheximide, and analyzed as in Figure 1C.

Cdc20-CB denotes the Cdc20-R145D allele. Cdc20-R145D (Cdc20-CB) protein migrates

more slowly on an electrophoretic gel as compared to wild type Cdc20. **(D)** ZZ-tagged

unlabeled Cdc20 wildtype, C-Box mutant I147A, P148A (Cdc20-CB) or IR mutant I609A, R610A (Cdc20-IR) or a mock purification from IVT lysate with no Cdc20 (-) was

pre-incubated with APC (5 nM) and ZZ-tagged ³⁵S-Securin generated by IVT. After a 15 min preincubation, E1/E2(Ubc4)/Methyl-Ubiquitin mix was added and ubiquitination

reactions were performed for the indicated times. See also Figure S1.

Figure 3. The majority of Cdc20 turnover occurs by the Cdc20^{cis} mechanism. **(A)** Asynchronous *pds1Δ clb5Δ SIC1^{10x}* cells were analyzed as in Figure 2C. Cdc20-CB denotes the Cdc20-R145D, IRΔ allele. Bands represented by Cdc20 and Cdc20-CB are indicated. Two exposures are shown. **(B)** ZZ-tagged ³⁵S-Cdc20 C-Box, IR mutant (I147A, P148A, I609A, R610A) or ³⁵S-Cdc20 C-Box, IR, D-box mutant (I147A, P148A, I609A, R610A, R17A, L20A) mutant was incubated with recombinant Cdh1, APC (1 nM), and E1/E2(Ubc4)/Methyl-Ubiquitin mix for the indicated times. **(C)** IVT generated ZZ-tagged ³⁵S-Cdc20 mutants, as in Figure 3B, were incubated with APC (5 nM), E1/E2(Ubc4)/Methyl-Ubiquitin mix, and with or without IVT-generated ZZ-Tagged unlabeled Cdc20 for the indicated times. **(D)** Asynchronous *pds1Δ clb5Δ SIC1^{10x}* cells were treated with cycloheximide and examined as in Figure 2C. Bands labeled Cdc20* are Cdc20 or Cdc20-D-box allele (*cdc20*-R17A, L20A), whereas Cdc20-CB* indicates the Cdc20-IRΔ, R145D allele or Cdc20-R145D, IRΔ, D-box (R17A, L20A) allele. **(E)** Securin and Cdc20 ubiquitination assays as in Figure 2B, except that APC was purified from *DOC1 cdh1Δ* or *doc1-4A cdh1Δ* strains.

Figure 4. Cdc20 levels oscillate with the cell cycle in a Cdh1- and transcription-independent manner. **(A)** Asynchronous *cdc15-2* or *cdc15-2 cdh1Δ* cells were arrested at 37°C and released into 23°C media. Time points were taken every 20 min. A sample of each asynchronous (Asy) culture and a *cdc20Δ* mutant are shown for reference. **(B)** *cdc15-2 TEF1p-CDC20* or *cdc15-2 TEF1p-CDC20 cdh1Δ* strains were arrested and released as in Figure 4A. Time points were taken every 10 min. Western blots were performed with the indicated antibody. See also Figure S2.

Figure 5. Cdc20^{cis} mechanism is inhibited by high substrate concentrations **(A)** ZZ-tagged unlabeled Cdc20 generated by IVT was pre-incubated with APC (5 nM) and the specified concentration of the Securin/Pds1 fragment (referred to as Securin 1-110; values represent the final assay concentrations). After a 15 min preincubation, E1/E2(Ubc4)/Methyl-Ubiquitin mix and ZZ-tagged ³⁵S-Securin generated by IVT was added and ubiquitination reactions were performed for 10 min. **(B)** ZZ-tagged unlabeled Cdc20 or ³⁵S-Cdc20 generated by IVT was pre-incubated for 15 min with APC (5 nM) and 10 μM Securin 1-110. For securin ubiquitination, E1/E2(Ubc4)/Methyl-Ubiquitin mix and ZZ-tagged ³⁵S-Securin generated by IVT was added for 10 min. For autoubiquitination, E1/E2(Ubc4)/Methyl-Ubiquitin mix was added for 10 min.

Figure 6. Model demonstrating how Cdc20^{cis} may be regulated by substrate. Red, purple, blue and green boxes represent the D-boxes, the C-box, the WD40, and the C-terminal IR of Cdc20, respectively (see Figure 1A).

Figure 1

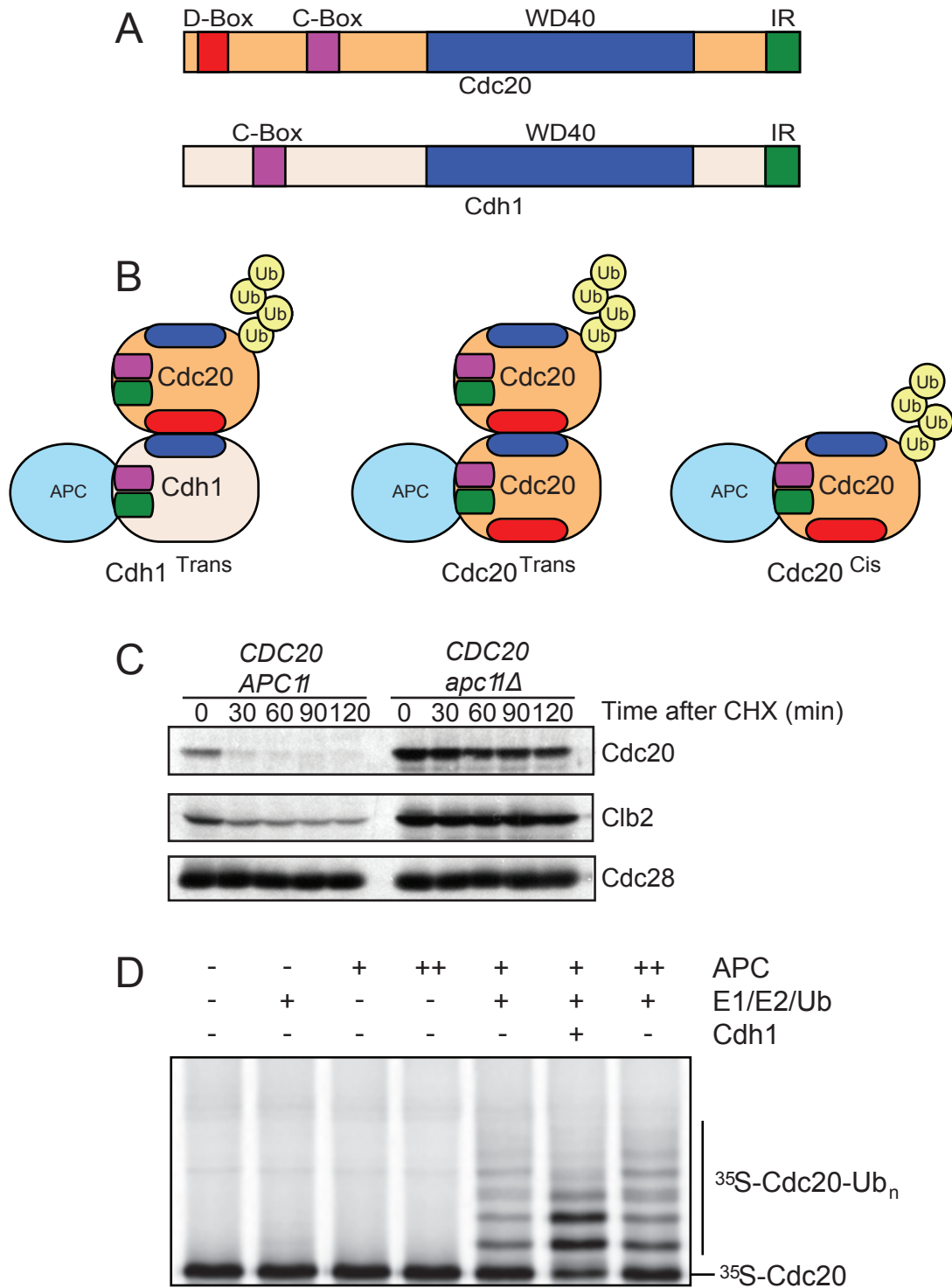
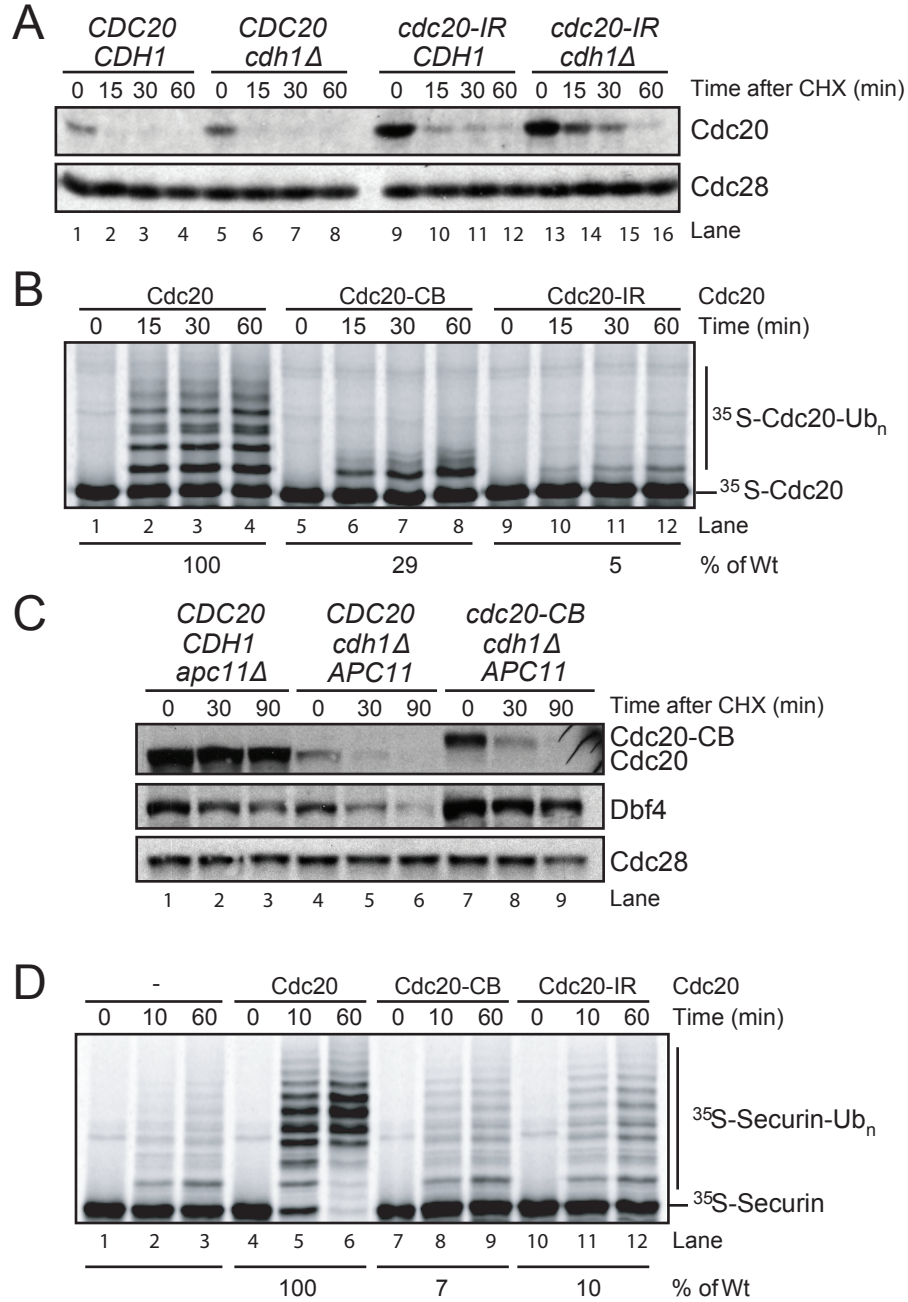


Figure 2



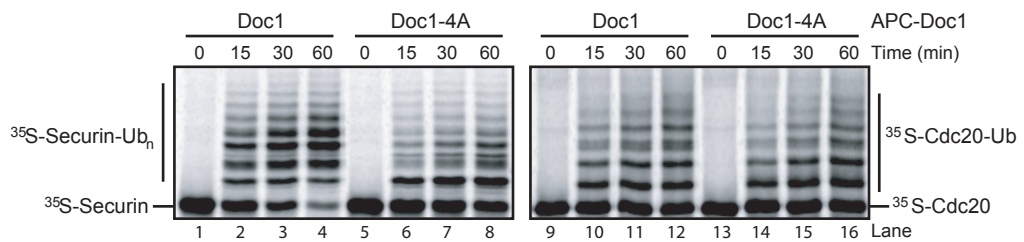
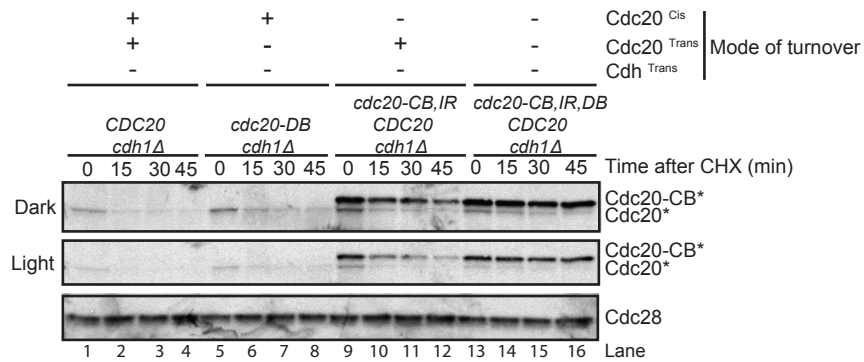
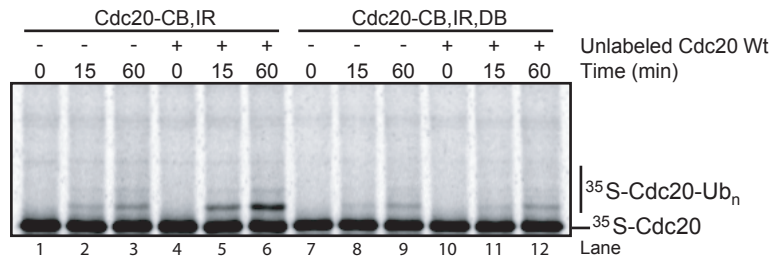
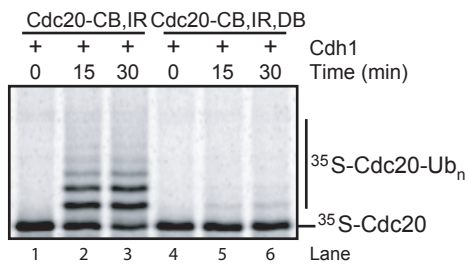
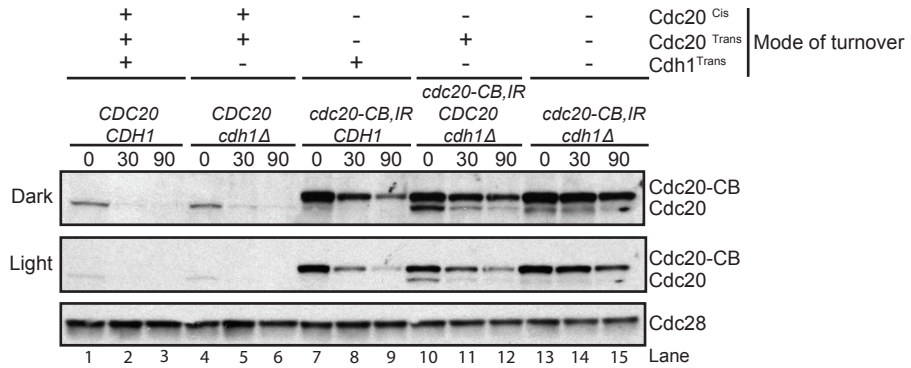


Figure 4

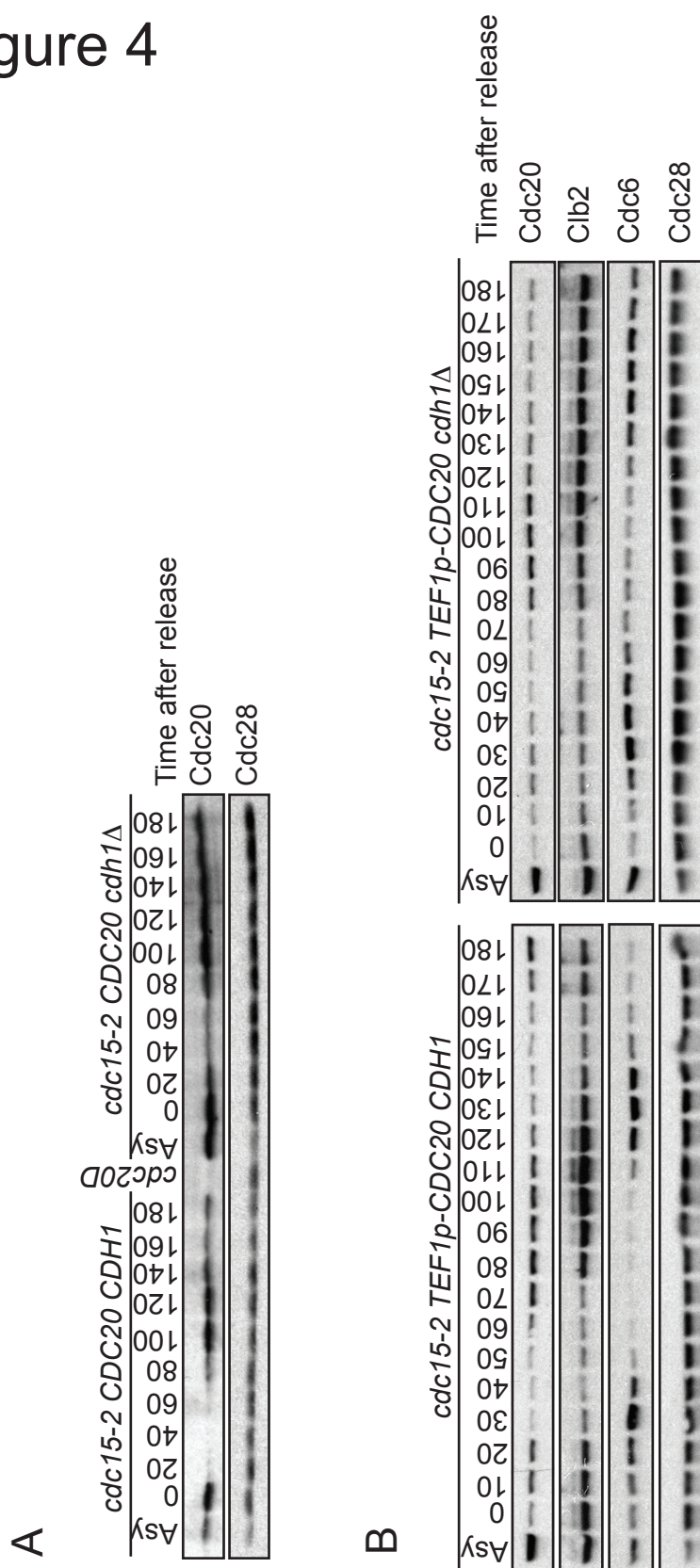


Figure 5

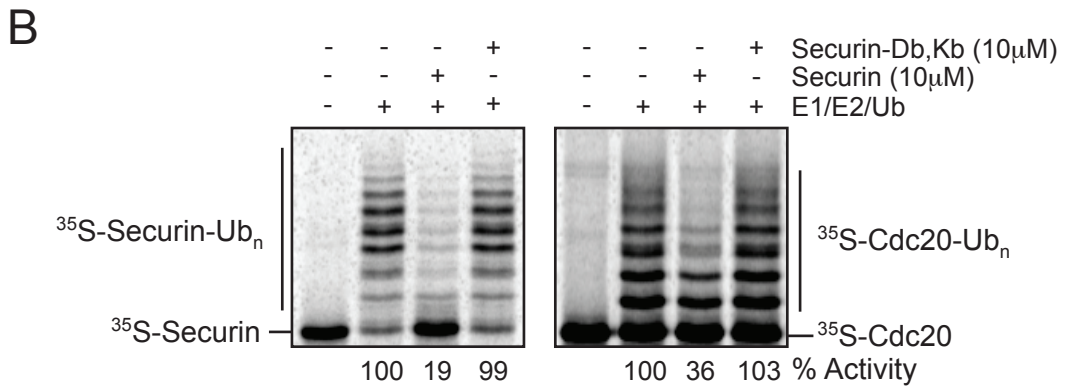
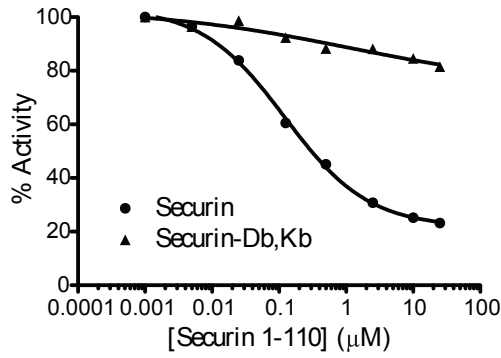
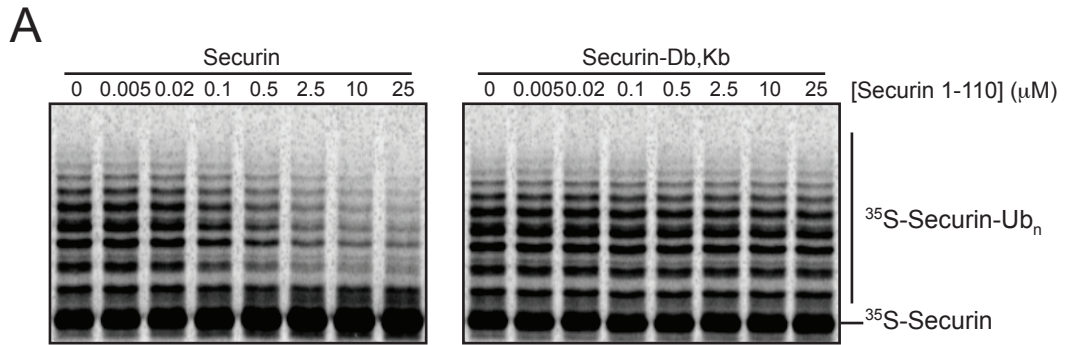
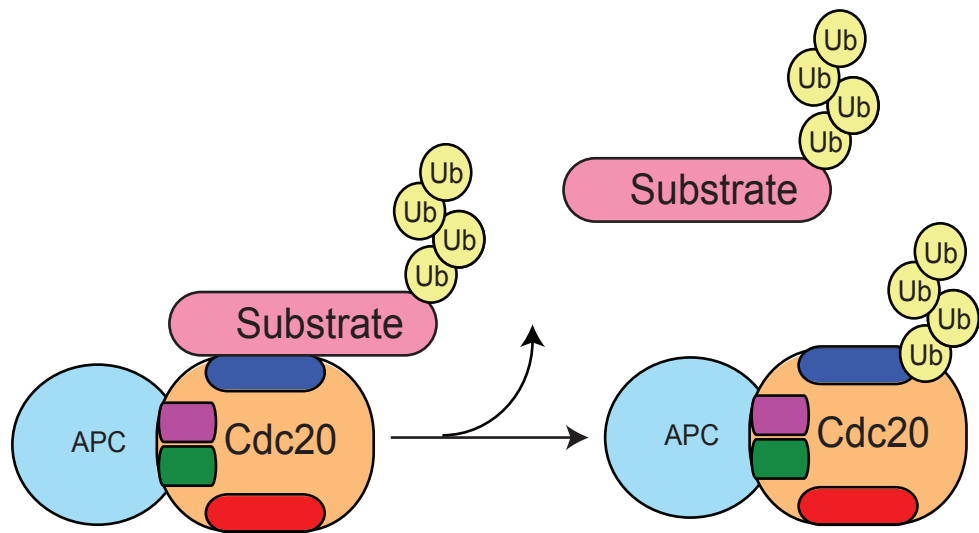


Figure 6

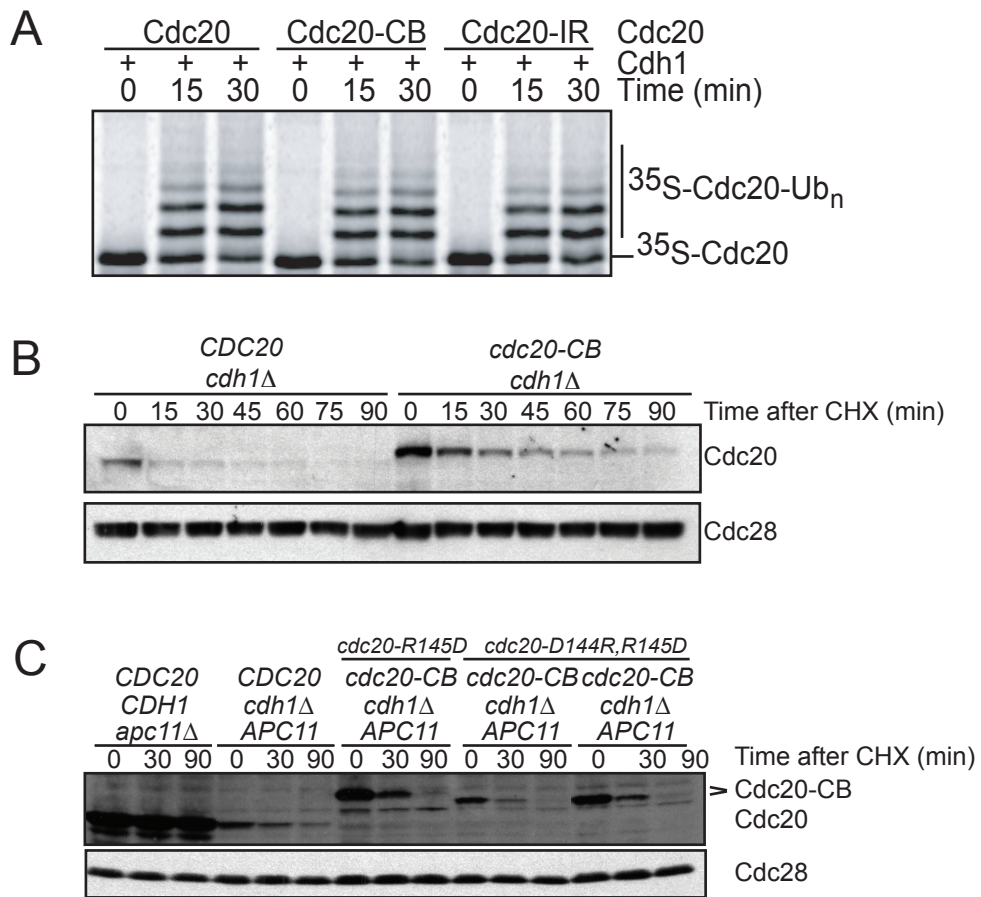


Supplementary Figure Legends

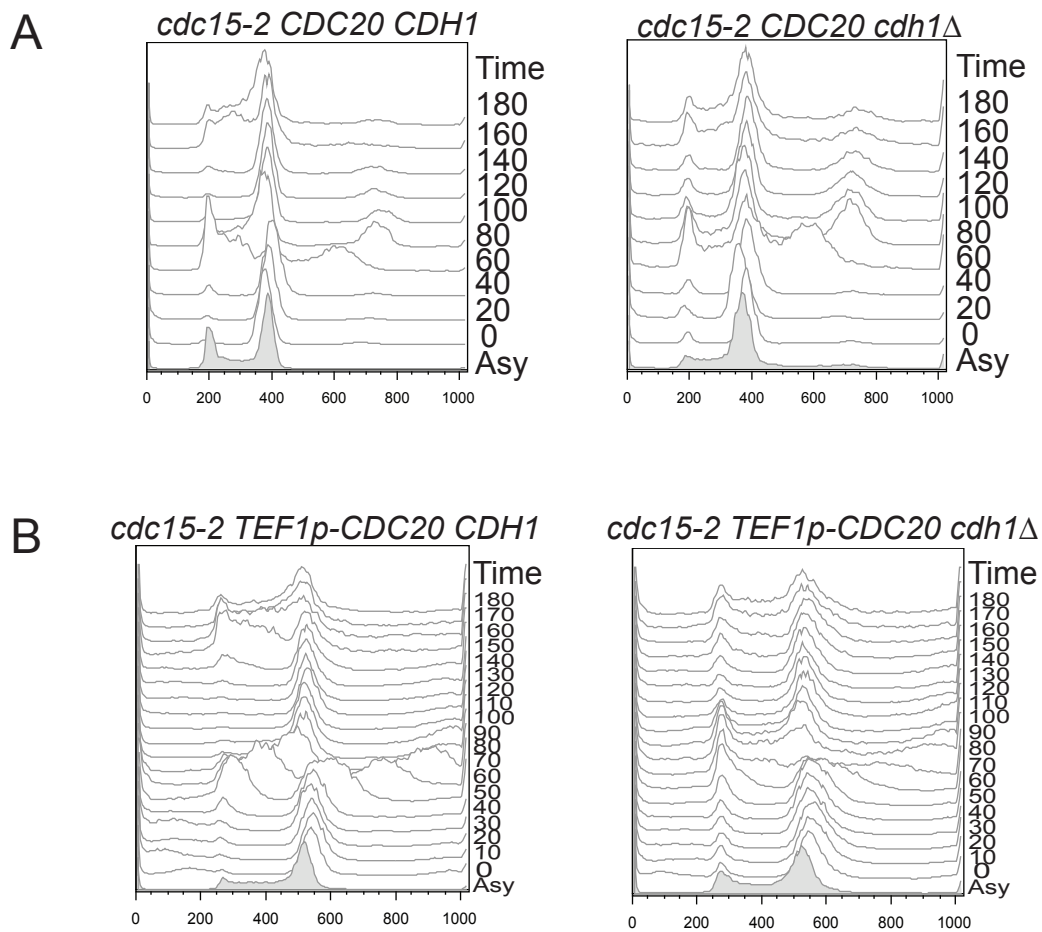
Figure S1. (A) *In vitro* Cdc20-IR and Cdc20-CB ubiquitination by Cdh1. ZZ-tagged ³⁵S-Cdc20 Wildtype, C-Box mutant (I147A, P148A; Cdc20-CB) or IR mutant (I609A, R610A; Cdc20-IR) was incubated with recombinant Cdh1 and APC (1 nM) for the indicated times. (B) Cdc20-R145D turns over relatively fast. Asynchronous *pds1Δ clb5Δ SICI^{10x}* cells were treated with cycloheximide, and analyzed as in Figure 2C. Cdc20-CB indicates the Cdc20-R145D allele. (C) Cdc20-D144R, R145D turned over with similar kinetics to Cdc20-R145D. Cycloheximide was added to asynchronous *pds1Δ clb5Δ SICI^{10x}* cells and samples were taken at indicated time points after addition. Cdc20-CB indicates the 3HA-Cdc20-R145D mutant or the 3HA-Cdc20-D144R, R145D mutant. Cdc28 is shown as a loading control. Two independent *cdc20-D144R, R145D* isolates are shown, blot was cropped to remove lanes between isolates.

Figure S2. Flow cytometry profiles for the experiments in Figures 4A and 4B. (A) Samples were taken at the same time as the protein samples in Figure 4A (20 min time points). (B) Samples were taken at the same time as the protein samples in Figure 4B (10 min time points).

Supplemental Figure 1



Supplemental Figure 2



Chapter 2

Apc1 is target of the DNA damage checkpoint

Abstract

The transition from metaphase to anaphase is one of many regulated steps throughout the cell cycle. This transition is controlled by an E3 ubiquitin ligase called the Anaphase Promoting Complex. When cells experience damage to their DNA they activate a checkpoint called the DNA damage checkpoint. This checkpoint arrest cells in metaphase, partially through the stabilization of an APC substrate. Here we provide evidence that the APC itself is a target of the DNA damage checkpoint. Importantly we show that the DNA damage checkpoint inhibits APC activity.

Introduction

Mitosis is an incredibly complex event, and as such cells have evolved many mechanisms to ensure that it occurs correctly. One point in mitosis that is highly regulated is the transition from metaphase to anaphase. The metaphase to anaphase transition is controlled by a multi subunit E3 ubiquitin ligase called the Anaphase Promoting Complex (APC)[7, 10, 32]. The APC is activated by the binding of the APC's two mitotic substrate receptors (Cdc20 and Cdh1) [3-5]. The activation of the APC at the metaphase to anaphase transition leads to the ubiquitination of both Pds1 and the mitotic cyclins[6, 7], which sets in motion a series of events that trigger the onset of anaphase[8].

Because of the importance of the APC in controlling this transition, a lot of work has been done in an attempt to understand how the APC functions. Previous genetic and structural work shows that the core APC, while composed of at least 13 subunits[1], can be broken down into 3 sub-complexes (the platform, the TPR subcomplex, and the catalytic subcomplex)[9, 10] (Figure 7A). The platform is composed of Apc1, Apc4, and

Apc5[9, 10]. Apc1 is the largest APC subunit[55], and contains a C-terminal motif called the Proteasome/Cyclosome repeats (PC repeats)[56]. The exact function of the repeats is unknown, however, recent structural work indicates they may be involved in binding Apc2, a member of the catalytic subcomplex [9]. The catalytic subcomplex is composed of the cullin Apc2, the ring Apc11, and the processivity factor Doc1 [9, 10, 16, 34], which is thought to form a bipartite substrate recognition motif with the APC's activators (Figure 7A) [13, 15]. In addition to binding the catalytic subcomplex, the platform also binds the TPR subcomplex. Previous work has shown that Apc4 and Apc5 along with Apc1 bind Cdc23, a member of the TPR subcomplex [10]. The TPR subcomplex is largely composed of the Tetratricopeptide (TPR) repeat proteins (Cdc23, Cdc16, and Cdc27) [10, 12]. This subcomplex is believed to function in binding the activators Cdc20 and Cdh1 (Figure 7A) [16, 17].

The APC, while essential for onset of Anaphase, is not the only enzyme involved in regulating this transition. When cells encounter DNA damage they activate the DNA damage checkpoint. This checkpoint has many functions, one of which is arresting damaged cells in metaphase [57]. The exact mechanism behind how this arrest is mediated is not well understood. What is known is that when cells detect DNA damage they activate a kinase called Mec1 [58] which is necessary for the arrest (*mec1Δ* cells fail to arrest) in metaphase on damage [59]. Mec1, once active, phosphorylates and activates the effector kinases Chk1 and Rad53 (Figure 7B) [57]. Both Chk1 and Rad53 are necessary, however, neither kinase is sufficient to arrest cells in metaphase. Both mutants pause in metaphase but eventually complete the cell cycle [59]. Previous work on the Chk1 branch of the pathway suggests that the APC substrate Pds1 is important for

this arrest [59-61] (Figure 7B). Phosphorylation of Pds1 by Chk1 is thought to increase the stability of Pds1 [59, 60] by inhibiting APC ubiquitination [62]. How phosphorylation of Pds1 accomplishes this is unknown. It is known, however, that the phosphorylations do not inhibit Pds1 binding to the APC [62]. The Rad53 branch of the pathway, unlike the Chk1 branch, is less understood. What is known is that Rad53, once activated, phosphorylates another kinase called Dun1 (Figure 7B). Once phosphorylated, Dun1 becomes active and [63, 64] then phosphorylates an unknown protein or proteins. It is believed that the target(s) of Dun1 are the substrates of the Rad53 branch that are involved in arresting cells [65] (Figure 7B). However, while Dun1 plays a role in arresting cells in metaphase, it is unknown if there are additional Rad53 substrates that are involved in enforcing the arrest.

Here we report that Apc1, a scaffolding subunit of the APC, is as a substrate of the DNA damage kinase Rad53. Importantly we also show that DNA damage checkpoint inhibits the turnover of several APC substrates including the APC activator Cdc20, in a Rad53 dependent manner. In addition, we demonstrate that the spindle assembly checkpoint (SAC) is activated by DNA damage and directly opposes the DNA damage checkpoint by turning over Cdc20. These data indicate a novel form of regulation in which the DNA damage checkpoint inhibits the APC during DNA damage.

Results

Apc1 is a target of the DNA damage checkpoint

On exposure to DNA damage, *Saccharomyces cerevisiae* activates a kinase cascade called the DNA damage checkpoint [57]. One of the major effects of this

checkpoint is a metaphase arrest. Previous work has indicated that the checkpoint kinases Chk1, Rad53 and Dun1 are involved in enforcing this arrest [59, 65]. While the Chk1 substrates have been identified [59, 61], the Rad53 and Dun1 target(s) of the checkpoint have proven to be more difficult to identify.

A recent screen was performed to look for proteins that change stability during DNA damage. The screen was performed by replacing endogenous promoters with the constitutive Translation Elongation Factor 1 promoter (pTef1). This was done so that any changes in protein levels were not due to transcriptional changes, but changes in protein stability. In addition to the replacement of the promoter, all the proteins were tagged with a C-terminal GFP tag. One intriguing hit from this screen was Apc1. While Apc1 levels did not drastically change on damage, Apc1 underwent an electrophoretic shift on an SDS page gel after DNA damage (Figure 8A). Similar shifts are often seen with targets of the DNA damage checkpoint and are a result of phosphorylation, which leads to decreased mobility on an SDS page gel. Previous work indicates that Apc1 in mammalian cells is highly phosphorylated in metaphase [66, 67]. Because of this, we sought to determine if the Apc1 shift we observed was dependent on the DNA damage checkpoint, or was a result of the cells being arrested in metaphase. To address this question we arrested cells in metaphase with nocodazole treatment and observed that Apc1-GFP did not change its mobility (Figure (8A)). This was encouraging, as it indicated that the shift seen on damage is likely due to the DNA damage checkpoint, not the cell cycle stage.

We next sought to determine if the shift observed for Apc1 was dependent on the DNA damage checkpoint itself. To examine this we generated strains containing the

pTef1-APC1-GFP allele along with deletions of the various DNA damage kinases. When we compared damaged to undamaged cells we saw that Apc1-GFP shifted on treatment with the DNA damaging agent Hydroxyurea (Hu) in wild type cells as previously shown (Figure 8B), however, in a *pTef1-APC1-GFP mec1Δ* strain the shift was abrogated (Figure 8B). This indicates that the shift was dependent on Mec1. The shift was also abolished in a *pTef1-APC1-GFP rad53Δ* strain (Figure 8B); indicating that the shift is also Rad53 dependent. This was intriguing, as it hinted that Apc1 might be a substrate of Rad53. While the experiment described above shows the shift is dependent on Rad53, it does not however, show that Apc1 is a direct target of Rad53. To examine if Apc1 was a direct of Rad53 we performed an *in vitro* phosphorylation assay. Using Flag purified Apc1, we observed *in vitro* incorporation of p32 labeled phosphate that was dependent on incubation with purified Rad53 (Figure 8C).

APC substrates are stabilized on DNA damage

This Apc1 result is intriguing as it indicates that Apc1 is likely a substrate of Rad53 and might be involved in arresting cells in metaphase. We hypothesized that the phosphorylation of Apc1 during damage might affect APC activity. To address this we performed cycloheximide chase assays and compared substrate stability in Hu treated cells to asynchronously growing cells. Similar to previous work we observed that Clb2 and Clb5 were both stabilized on treatment with damage (Figure 9A) [59, 68], and that two other APC substrates (Cdc5 and Dbf4) were also stabilized. Cdc20, unlike other APC substrates tested, was not completely stabilized by Hu treatment, consistent with previous results (Figure 9B) [23]. However, unlike previous results, Cdc20 turnover was

slightly retarded as compared to asynchronously growing cells. These results were intriguing as they hinted that the DNA damage checkpoint might be inhibiting APC function.

To determine if the stability seen on Hu treatment was dependent on the DNA damage checkpoint we performed cycloheximide chase assays after Hu treatment in *rad53Δ* and *dun1Δ* strains. Surprisingly, we found that the checkpoint mutants had no effect on stability when treated with Hu (Figure 9C). This result was puzzling; however, previous work has reported that the spindle assembly checkpoint (SAC) is activated by DNA damage [69]. The SAC is a checkpoint that inhibits the metaphase to anaphase transition. The SAC-based metaphase arrest is accomplished through the inhibition of the APC, via Cdc20 inhibition and degradation [26]. If the SAC is active in our Hu treated cells, it could explain the stability observed on Hu treatment both in wildtype cells and the checkpoint mutants.

To determine if the SAC was active in damaged cells and influencing APC activity we performed cycloheximide chase assays in *mad2Δ* strains. Mad2 is an important component of the SAC and is required for the SAC's metaphase arrest. When we compared substrate turnover in wildtype cells and *mad2Δ* cells during Hu treatment, we observed no effect on Cdc5 or Clb2 stability (Figure 9D). When we looked, however, at Clb5 turnover, we observed that Clb5 was no longer stabilized on Hu treatment in a *mad2Δ* (Figure 9D). In direct opposition to the Clb5 result, we observed that Cdc20 was very strongly stabilized in a *mad2Δ* when compared to wild type cells on Hu treatment

(Figure 9D). Importantly Cdc20 stability is not a function of the cells being *mad2Δ*, as asynchronously growing *mad2Δ* cells have no defect in Cdc20 turnover (Figure 9D).

Cdc20 stabilization in a *mad2Δ* during DNA damage is Rad53 dependent

The Cdc20 stability that we observed in *mad2Δ* cells indicates that cells exposed to DNA damage may inhibit the activity of the APC. We next sought to determine if this stability was dependent on the DNA damage checkpoint. We did this by generating a *mad2Δ mec1Δ* strain. We used this strain to perform cycloheximide chase assays during Hu treatment, and compared Cdc20 turnover in the double mutant to the *mad2Δ* strain. When we did this we found that Cdc20 was not stabilized in the double mutant (Figure 9A). This result indicates that the Cdc20 stability seen in the *mad2Δ* delete is dependent on Mec1. As Mec1 is the most upstream kinase in the DNA damage checkpoint pathway, we wanted to determine if other kinases in this pathway were also involved. We next looked at Cdc20 stability on Hu treatment in a *mad2Δ rad53Δ* double mutant. Cdc20, in this strain, also turned over with respect to the *mad2Δ* strain (Figure 9B). This indicates that Cdc20's stability is dependent on Rad53. We then sought to determine if Dun1 is important for Cdc20 stability in the *mad2Δ* strain. This was also done by generating a *mad2Δ dun1Δ* strain and looking at Cdc20 turnover. When we did this we saw no difference between the double mutant and the *mad2Δ* (Figure 9C). This result indicates that Dun1 is not involved in stabilizing Cdc20 on Hu treatment. Lastly we examined Chk1's role in stabilizing Cdc20 on damage. To test the contribution of Chk1, we generated a *mad2Δ chk1Δ* strain. Using this strain we were able to determine that the

Cdc20 stability on Hu treatment is also independent of Chk1. These results are consistent with the idea that Rad53 might be phosphorylating Apc1 and reducing APC activity.

Mapping Apc1 binding motifs

Previous work from our lab and structural analysis from the Barford lab has shown that Apc1 likely functions as a scaffold that brings together the TPR subcomplex and the catalytic subcomplex of the APC [9, 10]. While it is possible that phosphorylation of Apc1 blocks subcomplex binding, it seems unlikely, as Clb5 turns over in a *mad2Δ* on damage (Figure 9D), indicating that the APC is likely intact.

In an attempt to understand the function of Apc1 phosphorylation we set out to map the subcomplex binding sites on Apc1. To do this we generated a series of Apc1 truncation mutants and a partial deletion of Apc1's PC repeats. Using co-immunoprecipitation we were able to determine that Cdc16, one of the TPR subunits, is able to bind to 2 distinct fragments of Apc1: fragment 1-878, and fragment 1-1649 (Figure 10A and B). Previous work in our lab has shown that Apc4, Apc5 and Cdc23 are needed for an interaction between Apc1 and Cdc16 therefore these subunits are also likely to bind the above mentioned fragments [10]. These results provide strong evidence that the N-terminal half of Apc1 is involved in binding the TPR subcomplex. We next sought to determine where Apc2, a member of the catalytic subcomplex binds to Apc1. We found that only fragment 1-1649 was capable of binding to Apc2 (Figure 10A and B). This indicates that the catalytic arm of the APC binds most likely binds the C-terminal half of Apc1, as Apc2 does not bind to the 1-878 fragment. This is consistent with a

recent structure generated by David Barford's lab. In this structure Apc1's PC repeats are shown to closely interact with Apc2 [9].

Discussion

When yeast cells encounter DNA damage they activate a kinase cascade that, among other things arrests cells in metaphase. Previous work has shown that this arrest during damage is dependent on Mec1 [59]. Mec1 is able to activate two separate branches of the DNA damage checkpoint, each of which is essential for the prolonged arrest seen on damage [57-59]. One of the branches of this checkpoint is mediated through the kinase Chk1, and the other arm involves the kinases Rad53 and Dun1 [59, 65]. The substrate of the Chk1 path is known [60, 61], however, the target(s) of the Rad53 Dun1 pathway are currently unknown. Here we report that Apc1, one of the scaffolding subunits of the APC is a direct target of Rad53. This result is intriguing because it raises the possibility that the DNA damage checkpoint may inhibit APC activity, thus enforcing the metaphase arrest.

Previous work shows that both arms of the DNA damage pathway are necessary, but not sufficient, to maintain the arrest seen on DNA damage [59]. The finding that Apc1 is a Rad53 substrate is very interesting, as it helps to create a model for how the two branches of the checkpoint work together to arrest cells in metaphase. Chk1 is known to phosphorylate Pds1, an APC substrate [60, 61]. The destruction of Pds1 is one of the events that triggers anaphase onset [6]. The phosphorylation of Pds1 by Chk1 increases Pds1's stability [59, 60]. This increase in stability is caused by a decrease in the ability of the APC to ubiquitinate Pds1 [62]. How exactly this occurs is unknown. It

is known, however, that Pds1 phosphorylation does not affect Pds1 binding to the APC [62]. Phosphorylated Pds1 can still bind the APC, thus it is possible that given enough time, a small portion of bound Pds1 can be ubiquitinated by the APC and trigger anaphase onset. This would look very similar to what is seen in the *rad53Δ*, where only the Chk1 arm of the pathway is active. These cells initially arrest, however, the arrest cannot be maintained and cells eventually complete mitosis [59]. In a *chk1Δ*, much like in a *rad53Δ*, the cells also arrest and then eventually proceed to exit mitosis [59]. One possible explanation for the pause seen in *chk1Δ* cells is that the Rad53 phosphorylations on Apc1 decrease the activity of the APC. Decreasing the activity of APC would increase the half life of Pds1, slow the onset of anaphase, and result in the pause observed in a *chk1Δ* strain. The combination of Pds1 and Apc1 phosphorylations, however, may be sufficient to cause complete stabilization of Pds1 and arrest the cells in metaphase.

To determine if Apc1 phosphorylation has an effect on APC activity we performed a series of cycloheximide chase assays to look at the turnover of various APC substrate during damage. What we found was consistent with the idea that the APC is being inhibited. Many of the APC substrates that we looked at were completely stabilized on damage, consistent with previously reported results for two APC substrates; Clb2 and Clb5 [59, 68]. Also consistent with previous work, we found that Cdc20 turned over on Hu treatment [23]. Although, in our hands, Cdc20 turnover was slightly inhibited when compared to asynchronous cells. These results were encouraging, as they indicated that the DNA damage checkpoint might indeed be decreasing APC activity.

The results, however, did not show that the stability was dependent on the DNA damage checkpoint. To address this we performed cycloheximide chase assays in both *rad53Δ* and *dun1Δ* delete strains and looked at substrate stability. Every substrate we looked at in these mutants behaved the same on damage as in wildtype cells. This result was confusing, as it indicated that we might be on the wrong track. However, there have been reports that the SAC can be activated by DNA damage [69]. SAC activation could explain our observations. To see if the SAC was being activated we used a *mad2Δ* strain which is defective in SAC activity. Several of the substrates we looked at in the *mad2Δ* were still stable on damage including Cdc20, which was completely stable. This was interesting because it indicated that the SAC is actively turning over Cdc20 on damage, but that the DNA damage checkpoint is inhibiting APC activity and stabilizing Cdc20 along with other APC substrates.

Why the SAC is activated in these experiments is unknown. One possible explanation is that we are using Hu as the source of DNA damage. Hu causes damage by depleting the cellular dNTP pool thus blocking DNA replication. Inhibiting replication may lead to defects in centromere assembly; possibly failure to replicate centromeric DNA. These effects could result in the activation of the SAC. If this is the case, SAC activation would be dependent on the type of DNA damage.

The observation that the majority of APC substrates are stable on damage once the SAC is eliminated is consistent with a model where damage inhibits APC activity. To determine if the substrate stability observed in the *mad2Δ* was dependent on the DNA damage checkpoint, we generated double mutants where we deleted *mad2* and the

various checkpoint mutants to look at Cdc20 stability. In agreement with the model that Rad53 inhibits the APC during damage we observed that Cdc20 is unstable in the *mad2Δ mec1Δ* and *mad2Δ rad53Δ* strains. This turnover was not observed in the *mad2Δ dun1Δ* or the *mad2Δ chk1Δ* strains.

How Apc1 phosphorylation by Rad53 inhibits APC activity is unknown. However, we would like to propose a model for how this might occur. From the domain mapping data presented here (Figure 11), previous data from our lab [10], and the structure created by David Barford's lab[9], it seems likely that Apc1 functions as a scaffold for binding the TPR subcomplex and the catalytic subcomplex. The TPR subcomplex binds to the N-terminus of Apc1, and the catalytic subcomplex likely binds to the C-terminus of Apc1. Structural predictions of Apc1 indicate that between these two binding sites is a region that is highly unstructured [70]. This unstructured region is perfectly positioned to serve as a linker between the two halves of Apc1. We believe that this linker may position the two halves of Apc1 such that they promote interaction between the TPR subcomplex and the catalytic subcomplex to promote ubiquitination of Cdc20 and other substrates (Figure 11B upper panels). However, during DNA damage we propose that this linker is heavily phosphorylated by Rad53 (Figure 11B). In support of this argument the linker contains many serine and tyrosine residues (Figure 11A); both are residues that Rad53 is known to phosphorylate. We propose that phosphorylation of this linker changes the conformation of the APC. This conformational change might move the TPR subcomplex in such a way that it would no longer interact with catalytic subcomplex stabilizing Cdc20 and other APC substrates (Figure 11B bottom panels).

This model explains several pieces of data both presented here and in the literature. First as previously mentioned Pds1 phosphorylation does not affect the ability of Pds1 to bind to the APC as a substrate [62]. However Rad53 activity in cells inhibits Pds1 binding to the APC [62]. This result can be explained by our model. The APC uses a bipartite substrate recognition motif composed of the activators (which bind the TPR subcomplex) and Doc1 (catalytic subcomplex) to bind substrates [10, 13, 15-17]. When Rad53 phosphorylates the linker region on Apc1, the APC may undergo a slight conformational change such that Cdc20 and Doc1 are no longer positioned to correctly form the co-receptor, decreasing the APC's affinity for Pds1.

Additionally, we find in *mad2Δ* cells Clb5 is no longer stable on damage. This result appears to be in disagreement with the idea that the damage checkpoint inhibits APC activity. However, studies in yeast have shown that Clb5 may be different from canonical APC substrates. It has been reported that Clb5 turns over during the SAC, when the APC is thought to be inactive [71]. If this is true Clb5, recruitment to the APC is likely independent of Cdc20, as Cdc20 substrate binding during the SAC is inhibited [26]. How yeast Clb5 interacts with the APC in metaphase is unknown, however, evidence in mammalian cells suggests that Cyclin A, the mammalian Clb5 homologue, is brought to the APC via an interaction with Cyclin dependent kinase subunits (Cks) [72]. In yeast, Cks may also bring Clb5 to the APC. If this is true, it is likely that Cks1 presents Clb5 to the APC in a manner that is different from the normal way substrates are bound to the APC. Therefore Clb5 would not be affected by the conformational change that the Rad53 phosphorylations cause.

Much of this model is unproven, and more work still needs to be done to show if it is correct. Several key experiments remain to be done. For example *in vitro* kinase assays on APC1 fragments to map the phosphorylation sites, as it has proven to be very difficult to identify these sites by mass spectroscopy. If the residues in the linker region are indeed found to be the sites of phosphorylation, it will be imperative to mutate these sites and show that Rad53 no longer stabilizes Cdc20 and other APC substrates on damage. It will also be important to perform *in vitro* APC ubiquitination assays after Rad53 phosphorylation to show that the APC is inhibited.

Methods

Yeast Methods

Yeast were grown in Ym-1 media [52] and 2% dextrose. All cells were grown at 30°C unless otherwise noted. Strains used in Figures 8-10 are s288c strains with background *sml1* deletions. The strains used for Immuno-precipitation of the Apc1 fragments were A364a strains with background mutations in *pbr1* and *pep4*. Replacement of the APC1 promoter with *TEF1p* was accomplished using standard PCR-based techniques. All Tagging was done using standard techniques. Deletion strains were made by standard PCR based techniques and mutations were combined by crossing followed by tetrad dissection.

Damage and Cell cycle Arrest shift Assays

Cells were grown to saturation, diluted to an OD of .1 and allowed to grow for at least 2 doublings, cells were then split and diluted to an OD of 0.2. Asynchronous cells

were either allowed to grow in fresh media for 3 hours and 2 ODs cells were collected then spun down and washed in 1ml cold water. Cell pellets were then frozen on dry ice. Cells that were to be damaged were cut back to an OD of .2 and then grown in the presence of .2M Hu, or .05% MMS, or 2 μ g/ml 4NQO. Damaged cells were allowed to grow for 3 hours and were harvested as the asynchronous cells above. Cells arrested with Alpha factor were arrested at a concentration of 10 ng/ml. Cells that were arrested with nocodazole we arrested at 10ng/ml. Cells were processed as described below except that 7.5% pre-cast criterion gels were used to run that samples.

Half-life assays

Cells were grown to saturation, diluted to an OD of .1 and allowed to grow for at least 2 doublings, cells were then split and diluted into 2 cultures with an OD of .2. One culture was given fresh media and allowed to grow for 3 hours. The other culture was incubated in .2M Hydroxyurea for 3 hours. 2 ODs of cells were collected for the zero time point. Cell pellets were washed with 1 ml cold H₂O and frozen on dry ice. Cycloheximide was then added to cultures for a final concentration of 50 μ g/ml media. 2 ODs of cells were collected for each time point as indicated. Cell pellets processed as described below.

Western blots

Cell pellets were processed as follows. Cell pellets were thawed in boiling sample buffer (50mM Tris pH 7.5, 5% SDS, 5 mM EDTA, 10% Glycerol, 0.5% BME, 0.1 μ g/ml pepstatin A, 0.1 μ g/ml leupeptin, 0.1 μ g/ml bestatin, 0.1 mM Benzamidine, 5 mM NaF,

0.5 mM Na₃VO₄, 40 mM β-glycerophosphate, 1 mM PMSF). Cells were boiled for 5 min, followed by bead-beating 1.5 minutes. Samples were then spun and run on SDS page gels and transferred to nitrocellulose. Western blots were performed with low salt PBST (15 mM NaCl, 1.3 mM NaH₂PO₄, 5.4 mM Na₂HPO₄, 0.05% Tween pH 6.8). All primary antibody incubations were performed overnight in 5% milk and low salt PBST unless otherwise noted. Primary antibodies were used as follows: Cdc20 (yC-20) from Santa Cruz at 1:1000, Cdc28 from Santa Cruz (yC-20) at 1:1000, Dbf4 (yN-15) from Santa Cruz at 1:500, Clb2 (y180) from Santa Cruz 1:1000 Clb5 (yN19) from Santa Cruz at 1:500, Cdc5 (yN19) at 1:500 from Santa Cruz, Rad53 from the Durocher lab used at 1:1000, GFP (JL8) from Clontech used at 1:2000, HA from convance (HA.11 16B12) used at 1:2000, Dun1 (yN-19) 1:500 from Santa Cruz, the antibody pre-incubated with nitrocellulose several time over night to reduce background before use. Cdc16 from Heiter Lab used at 1:2000, Apc2 from the Heiter Lab used at 1:2500. Secondary antibodies used as follows. For Figures 8A and 8B, donkey anti-goat IgG-HRP (sc-2020) from Santa Cruz was used at 1:10,000, goat anti mouse (170-6516) from Bio-Rad used at 1:10,000. For Figures 9 and 10 bovine anti goat IgG-HRP (sc2350) from Santa Cruz was used at 1:10,000, and bovine anti rabbit IgG-HRP (Sc-2370) from Santa Cruz was used at 1:10,000. For Figure 11 Protein A, peroxidase conjugated (32400) from Pierce was used at 1:10,000, goat anti mouse (170-6516) from Bio-Rad used at 1:10,000.

Kinase Assay

Apc1-3xFlag cells were grown overnight to saturation and cut back the next morning to an OD of .1 cells were allowed to grow at least 2 doublings, and 800 ODs of

cells collected. Cells were washed with 10 mls cold water and frozen on dry ice. Cell pellet were thawed in 6ml of cold 1X lysis buffer (10% glycerol, 150 mM NaCl, 100mM Hepes Ph 8.0, .2% NP40, 1mM EDTA, 0.1 µg/ml pepstatin A, 0.1 µg/ml leupeptin, 0.1 µg/ml bestatin, 0.1 mM Benzamidine, 5 mM NaF, 0.5 mM Na₃VO₄, 40 mM β-glycerophosphate, 1 mM PMSF, 1 roche PhosStop tablet/10ml buffer and 1 roche EDTA free protease tablet/50ml buffer). Thawed cells were split into 8 tubes and ~500 µl of beads were added to each tube. Cells were bead beat for 1.5 minutes then incubated on ice for 5 minutes this was repeated until ~80% lysis. Lysates were cleared by spinning for 10 minutes at 14,000 rpms and 4°C. Supernatant was removed and incubated with pre-equilibrated Anti-Flag M2 magnetic beads (sigma) for 2 hours at 4°C. Beads were then washed 3X with a high salt lysis buffer (same as above except NaCl was used at 500mM). Beads were then washed 3X with cold kinase buffer (20mM Tris-Hcl Ph7.5, 20mM MgCl₂, 2mM MnCl₂, and 1mM DTT). Beads were then split, one tube was resuspended in 18µl kinase buffer. The other beads were resuspended in 15µl kinase buffer and 3µl TAP purified Rad53 kinase added. Rad53 was purified as previously described[53]. 1µl of adenosine 5' triphosphate γ^{32P} (~10µCi) (Perkin Elmer BLU002A250UC) was added to each reaction. Reactions were then incubated at 30° for 45 minutes. Reactions were then washed 3X with high salt lysis buffer described above. Reactions were then boiled in 10µl 2X Sina's sample buffer described in Chapter 1. Samples were run on a 4-20% precast criterion gel and exposed via autoradiograph.

Generation of the APC1 Fragment plasmids

All fragments were expressed from pRS426 plasmids that are under the control of the endogenous APC1 promoter and are all C-terminally tagged with 5HA. With the

exception of the fragment that contains a partial deletion of Apc1's PC repeats, the PC repeats have been replaced with 5HA. These constructs were all made using standard cloning techniques.

Fragment Immuno-precipitation Assays

Cells were grown overnight to saturation and cut back the next morning to an OD of .2 cells were allowed to grow at least 2 doublings, and 50 ODs of cells were collected for each strain. Cells were washed with 1 ml cold water and frozen on dry ice. Cell pellets were thawed in 750 μ l of cold 1X lysis buffer (10% glycerol, 150 mM NaCl, 50mM Hepes Ph 7.5, .4% Triton, 1mM EDTA, 0.1 μ g/ml pepstatin A, 0.1 μ g/ml leupeptin, 0.1 μ g/ml bestatin, 0.1 mM Benzamidine, 5 mM NaF, 0.5 mM Na₃VO₄, 40 mM β -glycerophosphate, 1 mM PMSF 1mM DTT. Thawed cells were lysed by bead beating for 1.5 minutes followed by 5 minutes on ice. This was repeated until cells were ~ 80% lysed. Lysates were cleared by spinning at 14,000 rpms at 4°C for 10 min. Supernatant was removed and incubated for 1 hour with 5 μ l of 12CA5 (mouse antibody against HA) for 2 hours at 4°C. Magnetic Protein A Dynabeads were added to the lysate/12CA5 slurry and were incubated for 1 hour at 4°C. Beads were then washed 3X with 1ml cold lysis buffer. Beads were then incubated with 30 μ l of 2X Sina's buffer at 65°C to elute bound protein. Samples were then run out on 4-20% pre-cast criterion gradient gel and transferred to nitrocellulose and probed via western as described above.

Figure legends

Figure 7 Diagram of the APC and the DNA damage checkpoint. **(A)** Diagram of the APC. Green subunits (Cdc27, Cdc16, and Cdc23) represent the TPR subcomplex. Blue subunits (Apc1, Apc4, and Apc5) represent the platform region. Red boxes in Apc1 represent the PC repeats. Orange subunit represents the activator (Cdc20 or Cdh1). Yellow subunits (Apc2, Apc11, and Doc1) represent the catalytic subcomplex. A blue substrate is bound by both Cdc20 and Doc1 via the bipartite co-receptor. Pink protein represents the charged E2 bound to Apc11, Red circle represents ubiquitin. **(B)** Diagram of the DNA damage checkpoint. Mec1 (gray), Chk1 (green), Rad53 (purple), Pds1 (light blue), Dun1 (brown) phosphates (Dark blue with white P) and unknown substrate of the Rad53 branch of the checkpoint (Red circle with ? mark)

Figure 8 Apc1 is target of the DNA damage checkpoint. **(A)** Apc1-GFP shifts on exposure to DNA damaging agents. Cells were incubated with alpha factor (G1 arrest) Nocodazole (metaphase arrest) and the following DNA damaging agents Hu, MMS and 4NQO. Rad53 blot is shown as damage control. **(B)** Western to determine if the Apc1-GFP shift is dependent on Mec1 and Rad53. Cells were grown in the presence or absence of Hu. Rad53 is shown to demonstrate that the *rad53Δ* status and that cells were damaged. **(C)** Apc1 is a direct substrate of Rad53. Apc1-3XFlag was purified from cells and incubated with P³² labeled ATP with and without active Rad53. Apc1 and Rad53 bands indicated by arrows.

Figure 9 APC substrates are stabilized during DNA damage. **(A)** APC substrates are stabilized during damage. Asynchronous and Hu treated cells were collected at indicated

time points after cycloheximide addition. Blots were probed with antibodies against Dbf4, Clb5, Clb2, Cdc5 and Cdc28, which served as a loading control. **(B)** Cdc20 is slightly stabilized by damage. Asynchronous and Hu treated cells were collected at indicated time points after cycloheximide addition. Blots were probed with antibodies against Cdc20, and Cdc28, which served as a loading control. **(C)** APC substrate stability in damage is not Rad53 or Dun1 dependent. Asynchronous and Hu treated cells were collected at indicated time points after cycloheximide addition. Blots were probed with antibodies against Cdc20, Clb5, Clb2, Cdc5 and Cdc28, which served as a loading control. Rad53 blot is shown as a control for the addition of damage and to confirm *rad53Δ* status. Dun1 blots are shown to confirm *dun1Δ* status. Genotypes of cells are indicated above time points. **(D)** Spindle assembly checkpoint is stabilizing Clb5 and turning over Cdc20 in Damage. Asynchronous and Hu treated cells were collected at indicated time points after cycloheximide addition. Blots were probed with antibodies against Cdc20, Clb5, Clb2, Cdc5 and Cdc28, which served as a loading control. Rad53 is shown as control for the addition of damage, and to confirm *rad53Δ* status. Genotypes indicated.

Figure 10 Cdc20 stability during damage is dependent on Rad53. **(A)** Cdc20 stability on damage is Mec1 dependent Asynchronous and Hu treated cells were collected at indicated time points after cycloheximide addition. Blots were probed with antibodies against Cdc20 and Cdc28, which served as a loading control. Genotypes indicated above time points. **(B)** Cdc20 stability on damage is Rad53 dependent. Asynchronous and Hu treated cells were collected at indicated time points after cycloheximide addition. Blots were probed with antibodies against Cdc20 and Cdc28, which served as a loading

control. Genotypes indicated above time points. **(C)** Cdc20 stability on damage is Dun1 independent. Asynchronous and Hu treated cells were collected at indicated time points after cycloheximide addition. Blots were probed with antibodies against Cdc20 and Cdc28, which served as a loading control. Genotypes indicated above time points. **(D)** Cdc20 stability on damage is Chk1 independent. Asynchronous and Hu treated cells were collected at indicated time points after cycloheximide addition. Blots were probed with antibodies against Cdc20 and Cdc28, which served as a loading control. Genotypes indicated above time points.

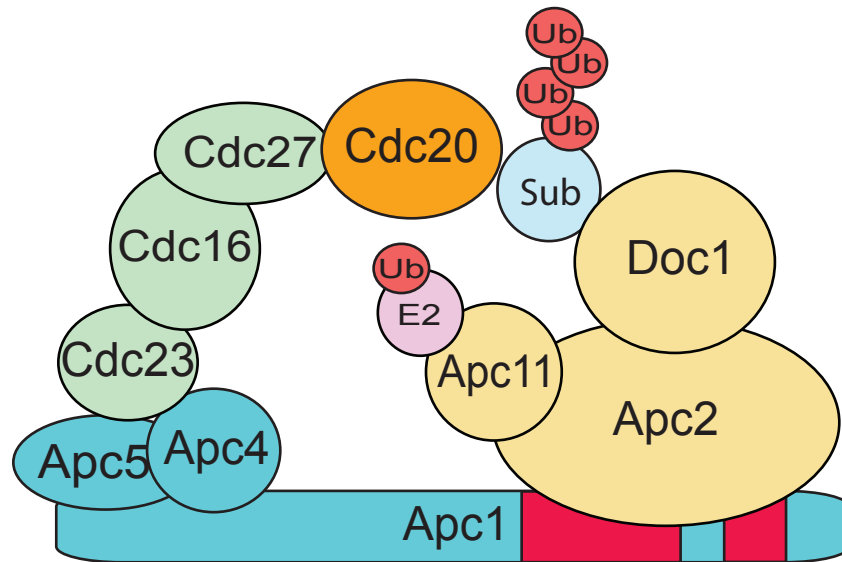
Figure 11 Apc1 Domain mapping **(A)** TPR subcomplex bind Apc1 in the N-terminus, the catalytic subcomplex binds the Apc1 C-terminus. HA-IP then westerns for Apc2 (catalytic subcomplex) and Cdc16 (TPR subcomplex). HA blot shows the amount of pulled down fragment. **(B)** Diagram showing results of Figure 11A. – indicates no binding + indicates binding.

Figure 12 Model for how damage may inhibit APC activity. **(A)** The linker region of Apc1. Amino acid sequence begins at 813 and ends at 915, Amino acid sequence below #s. H indicates predicted helix, C is a predicted coil. #'s underneath H and C represent confidence score, (low) 1-10 (high). O represents a predicted ordered residue, D represents disordered residue. #'s underneath O and D represent a confidence score (low) 1-10 (high). Figure taken from phyre [70] **(B)** Model for how Apc1 phosphorylation may inhibit APC activity. Teal rectangles indicated the two halves of Apc1 (left half (N-terminus, right half C-terminus), red stripes in Apc1 C-terminus indicate PC repeats. Green represents TPR subcomplex, yellow represents the catalytic subcomplex, orange

represents Cdc20, light blue represents substrate, red circle represent ubiquitin, and pink circle represent the charged E2. 4 ubiquitin molecules attached to the substrate indicates ubiquitination. Upper panels diagram normal turnover in the absence of damage with Cdc20 and substrate turning over. Bottom panels, the APC is inhibited by the phosphorylation (dark blue circles) of Apc1 between the N and C terminus. The change in the linker structure alters the confirmation of the APC and inhibits Cdc20 and substrate ubiquitination.

Figure 7

A



B

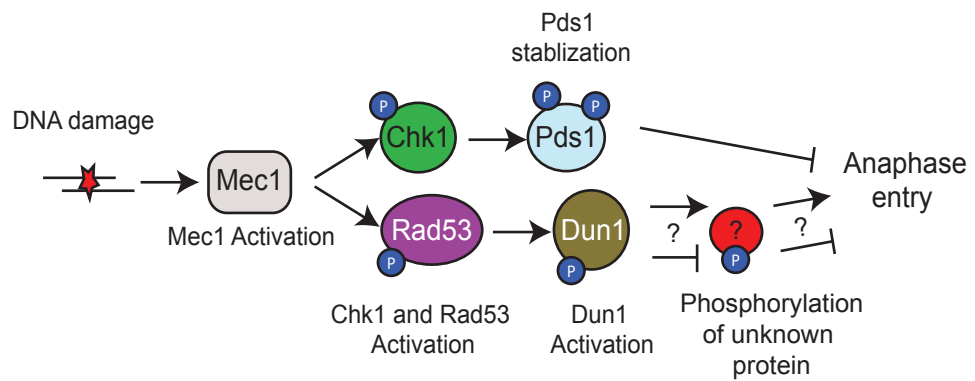


Figure 8

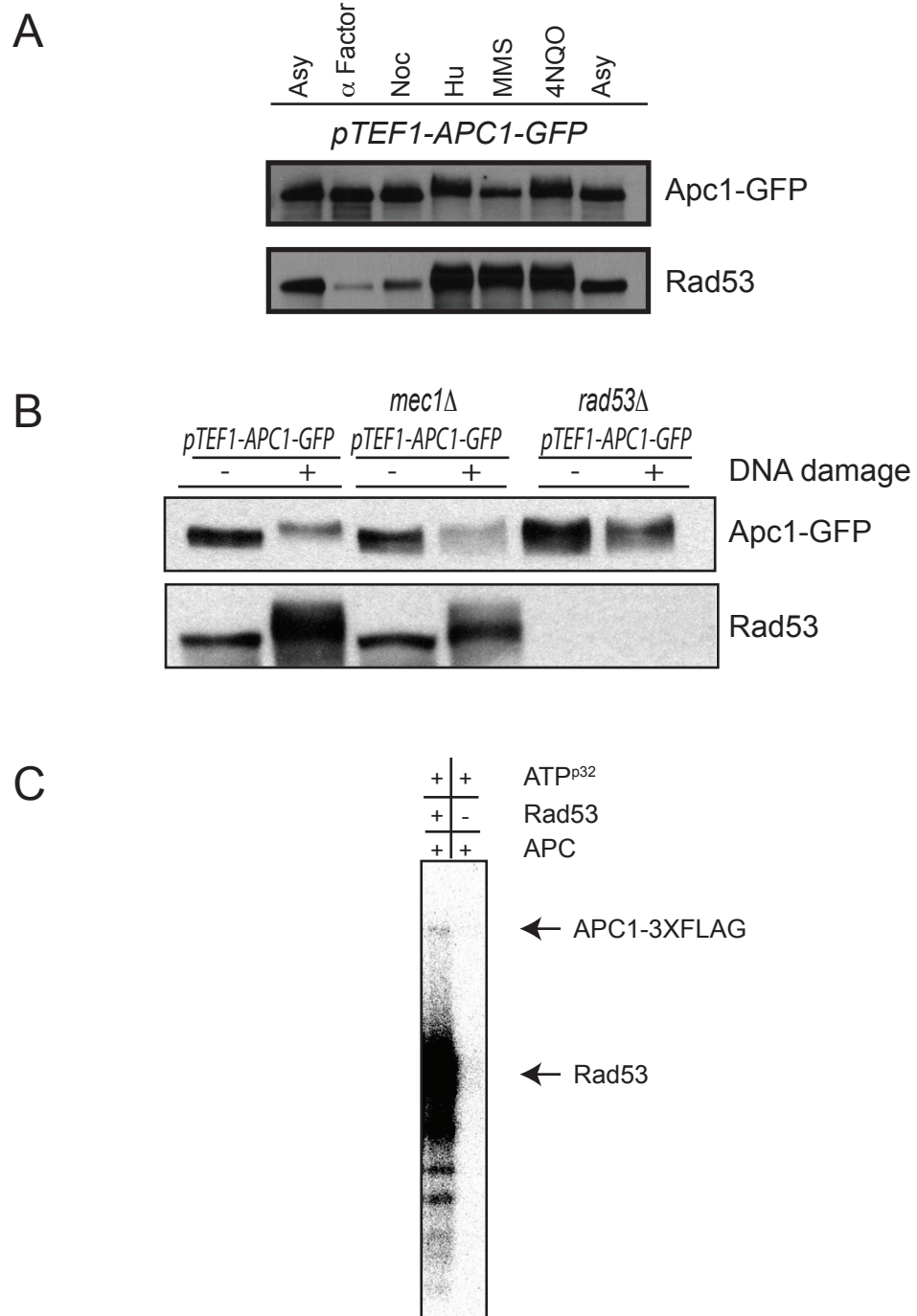


Figure 9

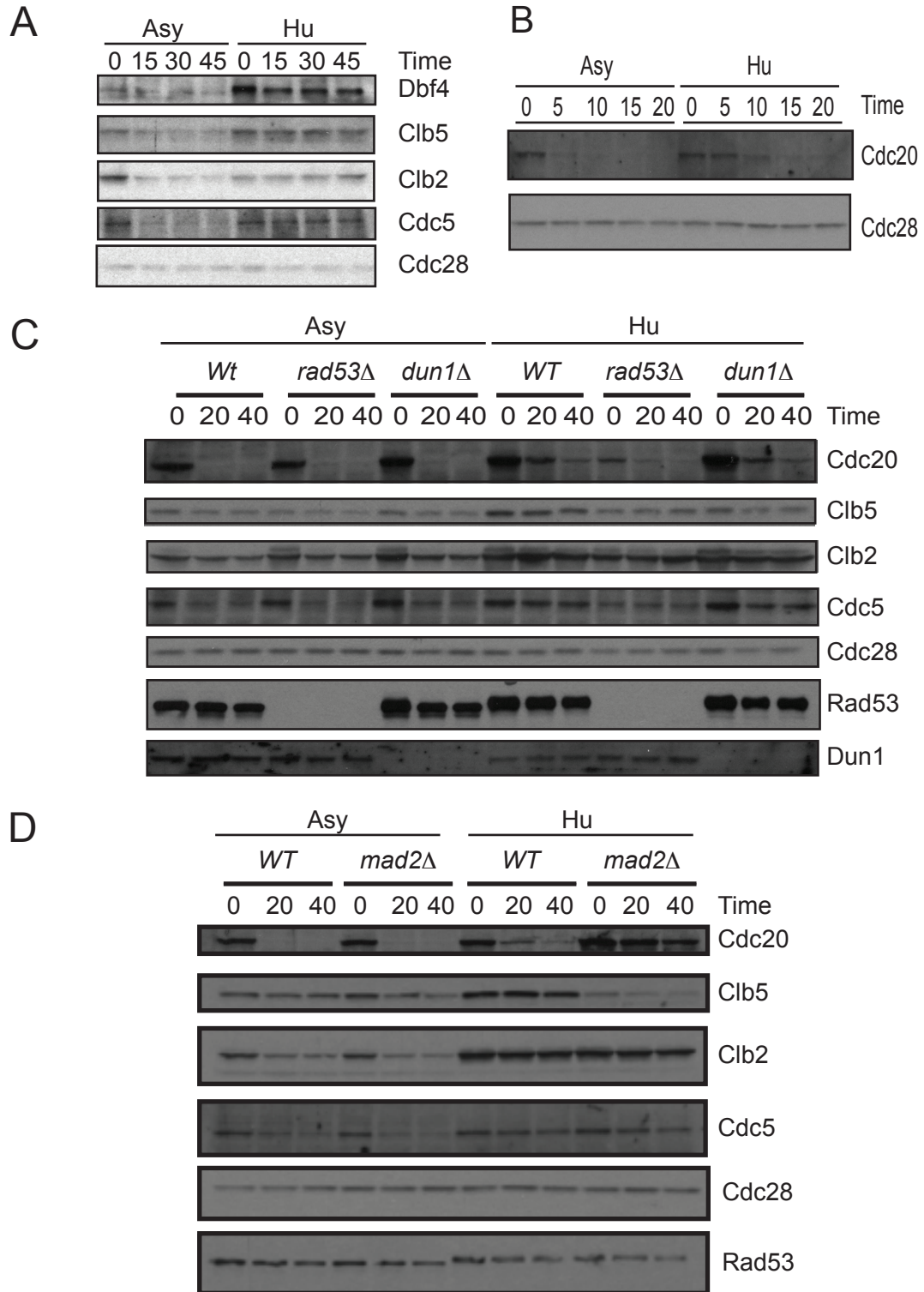


Figure 10

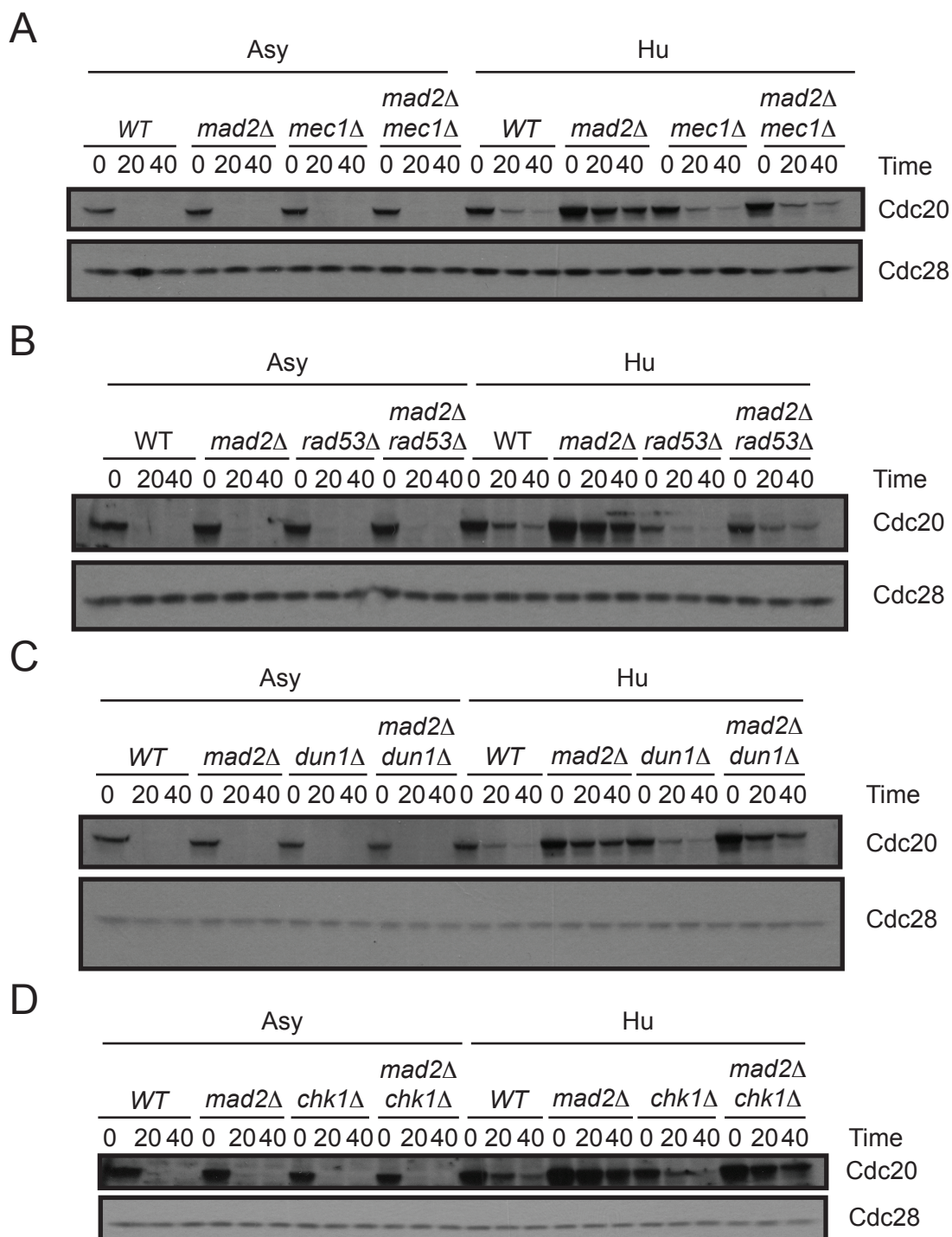
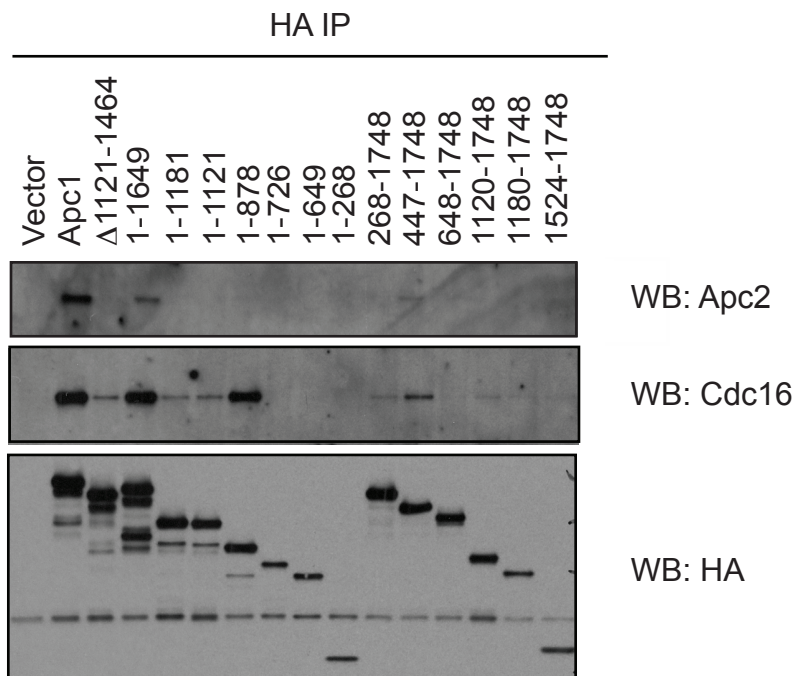


Figure 11

A



B

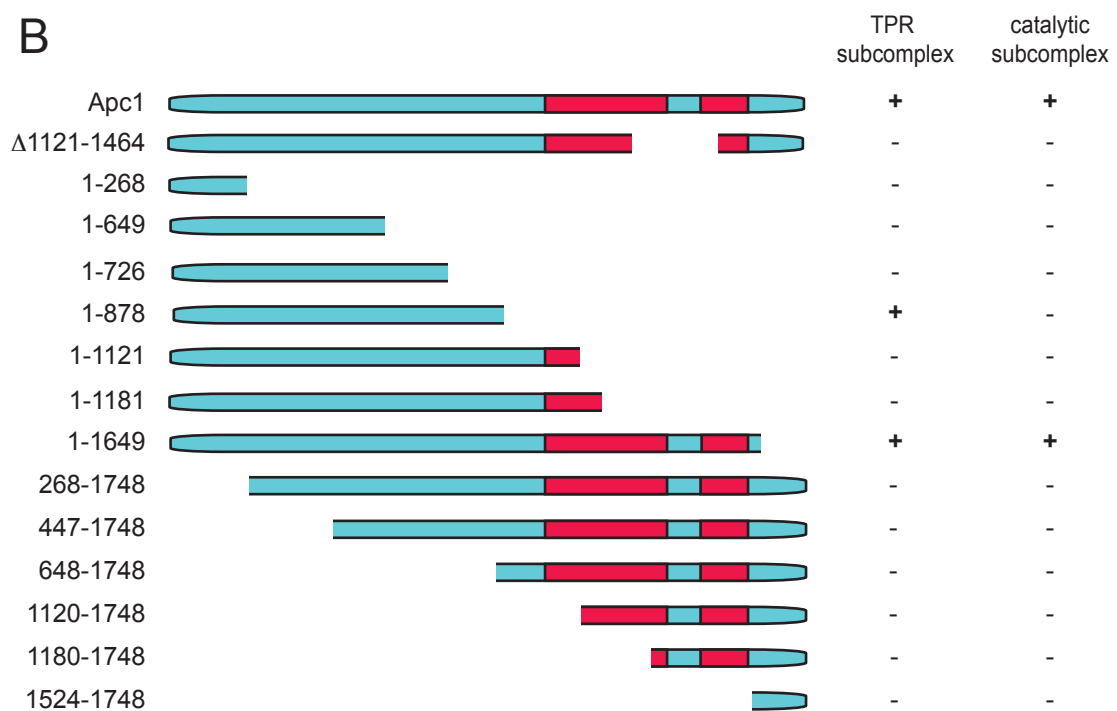
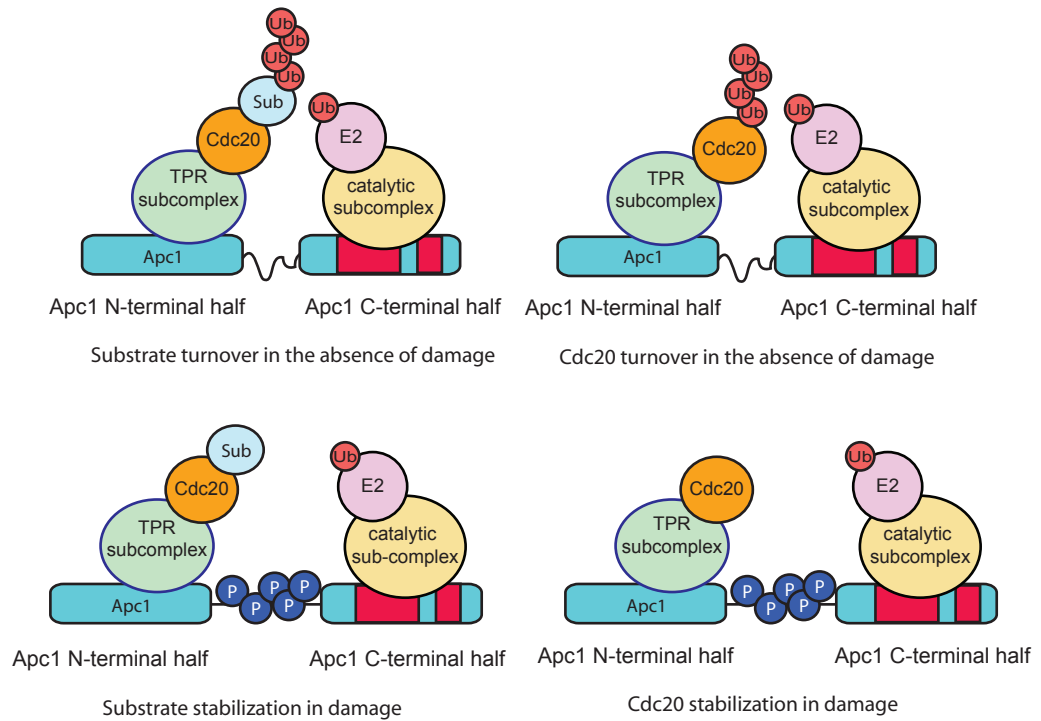


Figure 12

A



B



Work Cited

1. Yoon, H.J., Feoktistova, A., Wolfe, B.A., Jennings, J.L., Link, A.J., and Gould, K.L. (2002). Proteomics analysis identifies new components of the fission and budding yeast anaphase-promoting complexes. *Curr Biol* *12*, 2048-2054.
2. Passmore, L.A., Booth, C.R., Venien-Bryan, C., Ludtke, S.J., Fioretto, C., Johnson, L.N., Chiu, W., and Barford, D. (2005). Structural analysis of the anaphase-promoting complex reveals multiple active sites and insights into polyubiquitylation. *Molecular cell* *20*, 855-866.
3. Dawson, I.A., Roth, S., and Artavanis-Tsakonas, S. (1995). The *Drosophila* cell cycle gene *fizzy* is required for normal degradation of cyclins A and B during mitosis and has homology to the CDC20 gene of *Saccharomyces cerevisiae*. *The Journal of cell biology* *129*, 725-737.
4. Schwab, M., Lutum, A.S., and Seufert, W. (1997). Yeast Hct1 is a regulator of Clb2 cyclin proteolysis. *Cell* *90*, 683-693.
5. Visintin, R., Prinz, S., and Amon, A. (1997). CDC20 and CDH1: a family of substrate-specific activators of APC-dependent proteolysis. *Science (New York, N.Y)* *278*, 460-463.
6. Cohen-Fix, O., Peters, J.M., Kirschner, M.W., and Koshland, D. (1996). Anaphase initiation in *Saccharomyces cerevisiae* is controlled by the APC-dependent degradation of the anaphase inhibitor Pds1p. *Genes & development* *10*, 3081-3093.

7. Shirayama, M., Toth, A., Galova, M., and Nasmyth, K. (1999). APC(Cdc20) promotes exit from mitosis by destroying the anaphase inhibitor Pds1 and cyclin Clb5. *Nature* *402*, 203-207.
8. Oliveira, R.A., and Nasmyth, K. (2010). Getting through anaphase: splitting the sisters and beyond. *Biochemical Society transactions* *38*, 1639-1644.
9. Schreiber, A., Stengel, F., Zhang, Z., Enchev, R.I., Kong, E.H., Morris, E.P., Robinson, C.V., da Fonseca, P.C., and Barford, D. (2011). Structural basis for the subunit assembly of the anaphase-promoting complex. *Nature* *470*, 227-232.
10. Thornton, B.R., Ng, T.M., Matyskiela, M.E., Carroll, C.W., Morgan, D.O., and Toczyski, D.P. (2006). An architectural map of the anaphase-promoting complex. *Genes & development* *20*, 449-460.
11. Dube, P., Herzog, F., Gieffers, C., Sander, B., Riedel, D., Muller, S.A., Engel, A., Peters, J.M., and Stark, H. (2005). Localization of the coactivator Cdh1 and the cullin subunit Apc2 in a cryo-electron microscopy model of vertebrate APC/C. *Molecular cell* *20*, 867-879.
12. Lamb, J.R., Michaud, W.A., Sikorski, R.S., and Hieter, P.A. (1994). Cdc16p, Cdc23p and Cdc27p form a complex essential for mitosis. *The EMBO journal* *13*, 4321-4328.
13. Buschhorn, B.A., Petzold, G., Galova, M., Dube, P., Kraft, C., Herzog, F., Stark, H., and Peters, J.M. (2010). Substrate binding on the APC/C occurs between the coactivator Cdh1 and the processivity factor Doc1. *Nature structural & molecular biology* *18*, 6-13.

14. Carroll, C.W., Enquist-Newman, M., and Morgan, D.O. (2005). The APC subunit Doc1 promotes recognition of the substrate destruction box. *Curr Biol* *15*, 11-18.
15. da Fonseca, P.C., Kong, E.H., Zhang, Z., Schreiber, A., Williams, M.A., Morris, E.P., and Barford, D. (2011). Structures of APC/C(Cdh1) with substrates identify Cdh1 and Apc10 as the D-box co-receptor. *Nature* *470*, 274-278.
16. Passmore, L.A., McCormack, E.A., Au, S.W., Paul, A., Willison, K.R., Harper, J.W., and Barford, D. (2003). Doc1 mediates the activity of the anaphase-promoting complex by contributing to substrate recognition. *The EMBO journal* *22*, 786-796.
17. Vodermaier, H.C., Gieffers, C., Maurer-Stroh, S., Eisenhaber, F., and Peters, J.M. (2003). TPR subunits of the anaphase-promoting complex mediate binding to the activator protein CDH1. *Curr Biol* *13*, 1459-1468.
18. Schwab, M., Neutzner, M., Mocker, D., and Seufert, W. (2001). Yeast Hct1 recognizes the mitotic cyclin Clb2 and other substrates of the ubiquitin ligase APC. *The EMBO journal* *20*, 5165-5175.
19. Kimata, Y., Baxter, J.E., Fry, A.M., and Yamano, H. (2008). A role for the Fizzy/Cdc20 family of proteins in activation of the APC/C distinct from substrate recruitment. *Molecular cell* *32*, 576-583.
20. Kraft, C., Vodermaier, H.C., Maurer-Stroh, S., Eisenhaber, F., and Peters, J.M. (2005). The WD40 propeller domain of Cdh1 functions as a destruction box receptor for APC/C substrates. *Molecular cell* *18*, 543-553.
21. Glotzer, M., Murray, A.W., and Kirschner, M.W. (1991). Cyclin is degraded by the ubiquitin pathway. *Nature* *349*, 132-138.

22. Pflieger, C.M., and Kirschner, M.W. (2000). The KEN box: an APC recognition signal distinct from the D box targeted by Cdh1. *Genes & development* *14*, 655-665.
23. Prinz, S., Hwang, E.S., Visintin, R., and Amon, A. (1998). The regulation of Cdc20 proteolysis reveals a role for APC components Cdc23 and Cdc27 during S phase and early mitosis. *Curr Biol* *8*, 750-760.
24. Shirayama, M., Zachariae, W., Ciosk, R., and Nasmyth, K. (1998). The Polo-like kinase Cdc5p and the WD-repeat protein Cdc20p/fizzy are regulators and substrates of the anaphase promoting complex in *Saccharomyces cerevisiae*. *The EMBO journal* *17*, 1336-1349.
25. Foe, I.T., Foster, S.A., Cheung, S.K., DeLuca, S.Z., Morgan, D.O., and Toczyski, D.P. (2011). Ubiquitination of Cdc20 by the APC occurs through an intramolecular mechanism. *Curr Biol* *21*, 1870-1877.
26. Musacchio, A., and Salmon, E.D. (2007). The spindle-assembly checkpoint in space and time. *Nature reviews* *8*, 379-393.
27. Kim, H.S., Vassilopoulos, A., Wang, R.H., Lahusen, T., Xiao, Z., Xu, X., Li, C., Veenstra, T.D., Li, B., Yu, H., et al. SIRT2 maintains genome integrity and suppresses tumorigenesis through regulating APC/C activity. *Cancer cell* *20*, 487-499.
28. Rudner, A.D., and Murray, A.W. (2000). Phosphorylation by Cdc28 activates the Cdc20-dependent activity of the anaphase-promoting complex. *The Journal of cell biology* *149*, 1377-1390.

29. Zachariae, W., Schwab, M., Nasmyth, K., and Seufert, W. (1998). Control of cyclin ubiquitination by CDK-regulated binding of Hct1 to the anaphase promoting complex. *Science (New York, N.Y)* *282*, 1721-1724.
30. Jaspersen, S.L., Charles, J.F., and Morgan, D.O. (1999). Inhibitory phosphorylation of the APC regulator Hct1 is controlled by the kinase Cdc28 and the phosphatase Cdc14. *Curr Biol* *9*, 227-236.
31. Sudakin, V., Ganoth, D., Dahan, A., Heller, H., Hershko, J., Luca, F.C., Ruderman, J.V., and Hershko, A. (1995). The cyclosome, a large complex containing cyclin-selective ubiquitin ligase activity, targets cyclins for destruction at the end of mitosis. *Molecular biology of the cell* *6*, 185-197.
32. King, R.W., Peters, J.M., Tugendreich, S., Rolfe, M., Hieter, P., and Kirschner, M.W. (1995). A 20S complex containing CDC27 and CDC16 catalyzes the mitosis-specific conjugation of ubiquitin to cyclin B. *Cell* *81*, 279-288.
33. Thornton, B.R., and Toczyski, D.P. (2006). Precise destruction: an emerging picture of the APC. *Genes & development* *20*, 3069-3078.
34. Carroll, C.W., and Morgan, D.O. (2002). The Doc1 subunit is a processivity factor for the anaphase-promoting complex. *Nature cell biology* *4*, 880-887.
35. Yu, H. (2007). Cdc20: a WD40 activator for a cell cycle degradation machine. *Molecular cell* *27*, 3-16.
36. Manchado, E., Eguren, M., and Malumbres, M. (2010). The anaphase-promoting complex/cyclosome (APC/C): cell-cycle-dependent and -independent functions. *Biochemical Society transactions* *38*, 65-71.

37. Pesin, J.A., and Orr-Weaver, T.L. (2008). Regulation of APC/C activators in mitosis and meiosis. *Annual review of cell and developmental biology* 24, 475-499.
38. Robbins, J.A., and Cross, F.R. (2010). Regulated degradation of the APC coactivator Cdc20. *Cell division* 5, 23.
39. Lim, H.H., and Surana, U. (1996). Cdc20, a beta-transducin homologue, links RAD9-mediated G2/M checkpoint control to mitosis in *Saccharomyces cerevisiae*. *Mol Gen Genet* 253, 138-148.
40. Pan, J., and Chen, R.H. (2004). Spindle checkpoint regulates Cdc20p stability in *Saccharomyces cerevisiae*. *Genes & development* 18, 1439-1451.
41. Goh, P.Y., Lim, H.H., and Surana, U. (2000). Cdc20 protein contains a destruction-box but, unlike Clb2, its proteolysis is not acutely dependent on the activity of anaphase-promoting complex. *European journal of biochemistry / FEBS* 267, 434-449.
42. Thornton, B.R., and Toczyski, D.P. (2003). Securin and B-cyclin/CDK are the only essential targets of the APC. *Nature cell biology* 5, 1090-1094.
43. Zachariae, W., Shevchenko, A., Andrews, P.D., Ciosk, R., Galova, M., Stark, M.J., Mann, M., and Nasmyth, K. (1998). Mass spectrometric analysis of the anaphase-promoting complex from yeast: identification of a subunit related to cullins. *Science (New York, N.Y)* 279, 1216-1219.
44. Amon, A., Irniger, S., and Nasmyth, K. (1994). Closing the cell cycle circle in yeast: G2 cyclin proteolysis initiated at mitosis persists until the activation of G1 cyclins in the next cycle. *Cell* 77, 1037-1050.

45. Hayes, M.J., Kimata, Y., Wattam, S.L., Lindon, C., Mao, G., Yamano, H., and Fry, A.M. (2006). Early mitotic degradation of Nek2A depends on Cdc20-independent interaction with the APC/C. *Nature cell biology* 8, 607-614.
46. Matyskiela, M.E., and Morgan, D.O. (2009). Analysis of activator-binding sites on the APC/C supports a cooperative substrate-binding mechanism. *Molecular cell* 34, 68-80.
47. Spellman, P.T., Sherlock, G., Zhang, M.Q., Iyer, V.R., Anders, K., Eisen, M.B., Brown, P.O., Botstein, D., and Futcher, B. (1998). Comprehensive identification of cell cycle-regulated genes of the yeast *Saccharomyces cerevisiae* by microarray hybridization. *Molecular biology of the cell* 9, 3273-3297.
48. Zhu, G., Spellman, P.T., Volpe, T., Brown, P.O., Botstein, D., Davis, T.N., and Futcher, B. (2000). Two yeast forkhead genes regulate the cell cycle and pseudohyphal growth. *Nature* 406, 90-94.
49. Koranda, M., Schleiffer, A., Endler, L., and Ammerer, G. (2000). Forkhead-like transcription factors recruit Ndd1 to the chromatin of G2/M-specific promoters. *Nature* 406, 94-98.
50. Rape, M., and Kirschner, M.W. (2004). Autonomous regulation of the anaphase-promoting complex couples mitosis to S-phase entry. *Nature* 432, 588-595.
51. Burton, J.L., Tsakraklides, V., and Solomon, M.J. (2005). Assembly of an APC-Cdh1-substrate complex is stimulated by engagement of a destruction box. *Molecular cell* 18, 533-542.

52. Benanti, J.A., Cheung, S.K., Brady, M.C., and Toczyski, D.P. (2007). A proteomic screen reveals SCFGrr1 targets that regulate the glycolytic-gluconeogenic switch. *Nature cell biology* 9, 1184-1191.
53. Lopez-Mosqueda, J., Maas, N.L., Jonsson, Z.O., Defazio-Eli, L.G., Wohlschlegel, J., and Toczyski, D.P. (2010). Damage-induced phosphorylation of Sld3 is important to block late origin firing. *Nature* 467, 479-483.
54. Carroll, C.W., and Morgan, D.O. (2005). Enzymology of the anaphase-promoting complex. *Methods in enzymology* 398, 219-230.
55. Zachariae, W., Shin, T.H., Galova, M., Obermaier, B., and Nasmyth, K. (1996). Identification of subunits of the anaphase-promoting complex of *Saccharomyces cerevisiae*. *Science (New York, N.Y)* 274, 1201-1204.
56. Lupas, A., Baumeister, W., and Hofmann, K. (1997). A repetitive sequence in subunits of the 26S proteasome and 20S cyclosome (anaphase-promoting complex). *Trends in biochemical sciences* 22, 195-196.
57. Melo, J., and Toczyski, D. (2002). A unified view of the DNA-damage checkpoint. *Current opinion in cell biology* 14, 237-245.
58. Friedel, A.M., Pike, B.L., and Gasser, S.M. (2009). ATR/Mec1: coordinating fork stability and repair. *Current opinion in cell biology* 21, 237-244.
59. Sanchez, Y., Bachant, J., Wang, H., Hu, F., Liu, D., Tetzlaff, M., and Elledge, S.J. (1999). Control of the DNA damage checkpoint by chk1 and rad53 protein kinases through distinct mechanisms. *Science (New York, N.Y)* 286, 1166-1171.

60. Wang, H., Liu, D., Wang, Y., Qin, J., and Elledge, S.J. (2001). Pds1 phosphorylation in response to DNA damage is essential for its DNA damage checkpoint function. *Genes & development* *15*, 1361-1372.
61. Cohen-Fix, O., and Koshland, D. (1997). The anaphase inhibitor of *Saccharomyces cerevisiae* Pds1p is a target of the DNA damage checkpoint pathway. *Proceedings of the National Academy of Sciences of the United States of America* *94*, 14361-14366.
62. Agarwal, R., Tang, Z., Yu, H., and Cohen-Fix, O. (2003). Two distinct pathways for inhibiting pds1 ubiquitination in response to DNA damage. *The Journal of biological chemistry* *278*, 45027-45033.
63. Allen, J.B., Zhou, Z., Siede, W., Friedberg, E.C., and Elledge, S.J. (1994). The SAD1/RAD53 protein kinase controls multiple checkpoints and DNA damage-induced transcription in yeast. *Genes & development* *8*, 2401-2415.
64. Zhou, Z., and Elledge, S.J. (1993). DUN1 encodes a protein kinase that controls the DNA damage response in yeast. *Cell* *75*, 1119-1127.
65. Gardner, R., Putnam, C.W., and Weinert, T. (1999). RAD53, DUN1 and PDS1 define two parallel G2/M checkpoint pathways in budding yeast. *The EMBO journal* *18*, 3173-3185.
66. Steen, J.A., Steen, H., Georgi, A., Parker, K., Springer, M., Kirchner, M., Hamprecht, F., and Kirschner, M.W. (2008). Different phosphorylation states of the anaphase promoting complex in response to antimetabolic drugs: a quantitative proteomic analysis. *Proceedings of the National Academy of Sciences of the United States of America* *105*, 6069-6074.

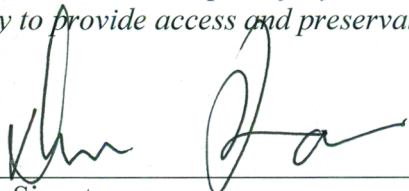
67. Kraft, C., Herzog, F., Gieffers, C., Mechtler, K., Hagting, A., Pines, J., and Peters, J.M. (2003). Mitotic regulation of the human anaphase-promoting complex by phosphorylation. *The EMBO journal* 22, 6598-6609.
68. Germain, D., Hendley, J., and Futcher, B. (1997). DNA damage inhibits proteolysis of the B-type cyclin Clb5 in *S. cerevisiae*. *Journal of cell science* 110 (Pt 15), 1813-1820.
69. Garber, P.M., and Rine, J. (2002). Overlapping roles of the spindle assembly and DNA damage checkpoints in the cell-cycle response to altered chromosomes in *Saccharomyces cerevisiae*. *Genetics* 161, 521-534.
70. Kelley, L.A., and Sternberg, M.J. (2009). Protein structure prediction on the Web: a case study using the Phyre server. *Nature protocols* 4, 363-371.
71. Keyes, B.E., Yellman, C.M., and Burke, D.J. (2008). Differential regulation of anaphase promoting complex/cyclosome substrates by the spindle assembly checkpoint in *Saccharomyces cerevisiae*. *Genetics* 178, 589-591.
72. Di Fiore, B., and Pines, J. (2010). How cyclin A destruction escapes the spindle assembly checkpoint. *The Journal of cell biology* 190, 501-509.

Publishing Agreement

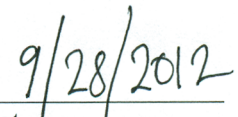
It is the policy of the University to encourage the distribution of all theses, dissertations, and manuscripts. Copies of all UCSF theses, dissertations, and manuscripts will be routed to the library via the Graduate Division. The library will make all theses, dissertations, and manuscripts accessible to the public and will preserve these to the best of their abilities, in perpetuity.

Please sign the following statement:

I hereby grant permission to the Graduate Division of the University of California, San Francisco to release copies of my thesis, dissertation, or manuscript to the Campus Library to provide access and preservation, in whole or in part, in perpetuity.



Author Signature



Date